Quantum and tensorial modeling of multipolar nonlinear optical chromophores by a generalized equivalent internal potential

Jason D. Weibel and David Yaron*

Department of Chemistry, Carnegie Mellon University Pittsburgh, PA 15213

Joseph Zyss†

Laboratoire de Photonique Quantique et Moléculaire, Institute d'Alembert,

Ecole Normale Supérieure de Cachan, Cachan, France

Abstract

The equivalent internal field model, originally developed for linear one-dimensional chromophores, is extended to three-dimensional multipolar chromophores. The extension requires two generalizations to the model. Firstly, the equivalent internal field must be generalized to an equivalent internal potential. Secondly, all tensor components of the hyperpolarizability must be taken into account. A general formalism is developed for analyzing the hyperpolarizabilities induced by application of various internal potentials to a molecular skeleton, assuming the hyperpolarizabilities are linearly related to the internal potential. This formalism utilizes a symmetry analysis, along with quantum chemical calculations done here with the Hückel, Pariser-Parr-Pople and INDO Hamiltonians and using single-configuration interaction (S-CI) theory. The formalism is applied to and tested on the benzene molecular skeleton. The hyperpolarizability is found to be linearly related to the internal potential provided the potential difference between carbon atoms is below a threshold of the order of 2eV. Various predictions of the model are tested against explicit calculations on *mono*-substituted, *ortho*-disubstituted, *meta*-disubstituted, and *tri*-substituted benzenes. For the substituents F, CH_3, OCH_3, OH and NH_2, many of the predictions of the equivalent internal potential model apply, indicating that the internal potentials arising from these substituents are in the linear regime. For the NO_2 and CN substituents, strong effects from nonlinear coupling are observed.

I. LIMITATIONS OF CURRENT MODELS TO ACCOUNT FOR THE TENSORIAL FEATURES OF THE NONLINEAR OPTICAL PROPERTIES OF MULTIPOLAR CHROMOPHORES

In a first generation of molecular engineering studies, the multi-dimensional nature of polarizable molecules in conjunction with the tensorial nature of their nonlinear optical properties had been largely overlooked. Indeed, until the early to mid-nineties, the main target had remained a quasi-one dimensional structure with basic rod-like features constraining polarizable electrons to oscillate along a one-dimensional channel. Donor and acceptor substituents at both ends of the rod provide the asymmetry and anharmonic electronic environment which are prerequisite towards quadratic nonlinear optical properties[1–5]. A bi-polar donor-acceptor intra-molecular conjugated molecule has thus emerged as the quasi-exclusive paradigm providing a generic blueprint to the field[6–8]. This avenue still inspires a wealth of interesting ongoing research, especially towards electrically poled electro-optic materials for subsequent application in communication devices[9,10]. Indeed, the relevance of this approach has been reinforced by the built-in potential of polar molecules to allow for electric field coupling and the subsequent macroscopic breaking of centrosymmetry both in solution (as in electric field induced second-harmonic generation, known as EFISH, for systematic evaluation of the magnitude of the β quadratic hyperpolarizability tensor) and in guest-host polymer films brought to a viscous glassy state by adequate temperature elevation (a crucial step towards the fabrication of thin film electrooptic materials). Moreover, an all-pervading two-level model[11,12] has further played a major role in outlining the necessity of polar features for quadratic nonlinear molecules, since it predicts a linear relation between β_{xxx}, the main component of the hyperpolarizability tensor along the charge transfer axis, and $\Delta\mu_x$, the difference between excited and ground state dipole moment in the two-level model. However, it was shown later[13–15] that the validity of the two-level model was strictly limited to 1-D tensorial systems if only for pure geometric reasons.

Finally, EFISH provides only $\vec{\beta}\cdot\vec{\mu}$ where β is the dipolar part of the tensor (with $(\vec{\beta})_i = \sum_j \beta_{ijj}$ and indices running over the three directions of Cartesian space) and it seemed only natural to focus on those quantities which were readily amenable to experimental observation. However, pioneering work by Maker et al.[16,17] had shown a different way of measuring β's by harmonic light scattering which, due to the non-coherent nature of such

process[18], did not impose on molecular solutions the constraint of centrosymmetry breaking. However, the potential of this work had remained largely ignored at the time until it was revived in the nineties under the different name of Hyper-Rayleigh scattering[19,20].

This bipolar target for nonlinear optics molecular engineering started to be challenged in the aftermath of a series of converging theoretical predictions and models as well as experimental observations throughout the nineties[21–29]. Indeed, emergence of a broader multipolar paradigm encompassing the earlier one as a special case has designated new directions for more elaborate molecular design, much beyond the cruder quasi-1-D template. The enlarged realm of multipolar molecules permits benefits from the three-dimensional nature of potential candidate molecules while fully exploiting the tensorial features of the associated optical properties. Limitations of the earlier dipolar approach has called for an extensive renewal of the enabling theoretical and experimental methodology towards measurements and poling techniques, as well as modeling of electronic and structural properties of multipolar molecules.

Ongoing propositions, synthesis and demonstrations of multipolar molecular design schemes result from a converging set of group theoretical, quantum mechanical and experimental efforts in both chemistry and physics which have jointly demonstrated the relevance of multiple charge transfer interactions mediated by 2- and 3-D polarizable electron systems. A major challenge is to enrich the tensorial character of the β hyperpolarizability beyond a unique "diagonal" β_{xxx} coefficient so as to allow for significant and possibly dominant "non-diagonal" β_{ijk} coefficients with i, j, and k along two and eventually three different directions of the molecular framework. Basic templates have been proposed along these lines in Ref. 22, a selection of which is highlighted in Fig. 1. An alternation of donor and acceptor groups at the corner of a cube provides a general template towards further chemical specification of 3-D octupolar systems, an important subset of multipolar systems whereby cancellation of the dipole moment is compatible with a non-centrosymmetric anharmonic structure. A single non-zero and eventually significant β_{xyz} coefficient (with x, y and z along the three axes of the cube) is attached to such a structure according to the requirements of a $\overline{4}3m$ type structure with such possible implementations as organo-metallic copper-bipyridine complexes[30] or substituted biphenyls[31]. For the most general 3-D octupolar structure, the symmetry constraints of the cubic structure can be relaxed to that of a triclinic rhombohedric structure containing three non-orthogonal twofold axes. Further crystalline level studies[32–34]

have shown crystalline engineering ways to direct the packing of 2- and 3-D octupoles in efficient crystalline lattices.

We concentrate in this work on a first generation of multipolar systems of two-dimensions such as multiply substituted aromatic systems. Consistence between 3- and 2-D multipolar architectures can be ensured by means of adequate space projections: for example the 2-D trigonal octupolar template in Fig. 1(b) can be generated by orthogonal projection of the 3-D octupolar cube along one of its main diagonals onto the corresponding perpendicular plane. Indeed, peripheral alternation of three identical donors together with a corresponding set of acceptor groups, both sets imparting three-fold symmetry to the aromatic ring, had been recognized since the beginning of this field as the simplest octupolar extension of the earlier D-π-A template and has served as a 2-D octupolar template[21,35]. Nevertheless, however interesting from a fundamental point of view, octupolar molecules seemed to lead to a practical dead-end in terms of usable nonlinear materials since the absence of a dipole moment precludes electric field coupling and the application of standard electric field poling techniques. Demonstration of tensorial statistical ordering by optical poling techniques[27,36,37] has then provided the "multipoling" enabling tool, moreover entailing many conceptual and practical advantages over the cruder electric field poling technique such as the possibility of controlling the imprinted tensorial multipolar pattern by the phase and polarization of the encoding laser beams.

A consistent multipolar engineering avenue all the way from molecules and materials to applications and devices[38–40] is being currently developed in different laboratories, obviously requiring that earlier foundations, sometimes elaborated more than two decades ago in the narrower realm of 1-D structures, be revisited.

One of such important earlier models is being referred to as the "Equivalent Internal Field" (EIF) which had proposed, along earlier lines set by Debye in the context of the static and linear properties of H-X molecules, to account for the emergence of a dominant β_{xxx} coefficient when grafting a substituent on an aromatic ring (the x axis going from the center of the ring to the substituted carbon site)[41,42]. The key approximation in this model consists in replacing the action of the substituent on the ring by an internal field which is responsible for polarizing the π electron system in conjunction with the externally applied field. Identification of the two equivalent systems, namely the actual substituted species and the aromatic ring embedded in the equivalent internal field can be simply shown to provide

the following linear relationship:

$$\beta_{xxx} = 3\left(\gamma^0_{xxxx} \Big/ \alpha^0_{xx}\right)\Delta\mu^0_x \,, \tag{1}$$

where γ^0_{xxxx} and α^0_{xx} stand for the cubic and linear polarizability tensor coefficients of the unsubstituted backbone while $\Delta\mu^0_x$ is the π electron dipole of the substituted molecule, sometimes referred to as the mesomeric moment. This relation has been validated by quantum mechanical calculations[43] as well as experiments for a number of singly substituted aromatic systems[11,12]. However, this approach entails a number of major drawbacks which precludes its application beyond a relatively narrow class of molecules. These are outlined in the following:

1) Even in the case of markedly unidirectional systems such as singly substituted aromatics, a purely 1-D model fails to account for the emergence of an accompanying "off-diagonal" β_{xyy} coefficient (with y in the aromatic plane and perpendicular to the x charge transfer axis). Such coefficients appear indeed, from both quantum calculations and experiments, to be of comparable magnitude to that of the "diagonal" β_{xxx} coefficient[14,27,28]. Moreover, the number of states required to provide a correct quantum picture of the complete tensorial features of nonlinear molecules has been shown to be larger than two, thus showing the limits of the 2-level model when tensorial anisotropy plays a role[13,14].

2) The EIF model brings in an oversimplification in the case of doubly substituted molecules, especially in *ortho* and *meta* position, whereby a single electric field cannot be expected to account for the relative positioning of a pair of substituents. Although a vectorial addition scheme of the fields associated to individual substituents is conceivable, such an additive linear assumption would not be applicable to strongly interacting substituent groups. More generally, the linear assumption underlying the EIF model is well known to break down at higher levels of charge transfer interaction, leading to the introduction of a dominant Mulliken-like charge transfer contribution to make up for the non-additive part of β according to $\beta_{xxx} = \beta^{EIF}_{xxx} + \beta^{CT}_{xxx}$[11,12]. As already mentioned, the additional β^{CT} term can be expressed by means of a two-level model albeit of validity restricted to quasi-1D systems which will not extend to multipolar systems. A

quantum n-level approach fully accounting for the tensorial properties of 2-D and 3-D octupolar systems has been recently developed[44].

3) A final drawback of the EIF method which served as the main incentive for this work was the obvious inadequacy of a field perturbation with vectorial features to account for an octupolar substitution pattern such as in Figs. 1 (b) and (c). Any perturbation scheme corresponding to the trigonal D_{3h} structure in Fig.1 (b) must reflect the symmetry of the substitution pattern which is by nature non-vectorial. In the case of weak to moderate coupling strengths, vectorial addition of the equivalent fields attached to individual substitution sites may perhaps permit a representation of the overall multiple substitution pattern. However, the overall coupling of the aromatic skeleton will then strictly vanish due to the threefold symmetry of the equivalent fields and the resulting cancellation of their vector sum.

The validity of the EIF model is thus tightly constrained by its built-in vectorial nature which precludes its utilization in more general situations whereby 2- and 3-D substitution patterns will trigger higher order components of the β tensor beyond purely vectorial ones. As will be outlined in this work, an effective electrostatic potential function associated to a given arbitrary substitution pattern and its subsequent expansion in terms of spherical harmonics, entailing the well known practical and conceptual advantages of rotational invariance based on a spherical tensor group representation, provides much broader foundations which are capable of encompassing a wealth of patterns beyond the grasp of the cruder vectorial EIF description (corresponding to first order truncation of the potential expansion).

We will therefore develop in Section II the basis of an Equivalent Internal Potential (EIP) model where the potential will appear as a powerful substitute to the field. The model can be further simplified by localization of the potential as on-site perturbations at discrete relevant substituent positions, allowing for straightforward implementation in the molecular quantum Hamiltonian at different levels of approximations as detailed in Section III. A full symmetry analysis is then provided in Section IV which evidences a general correspondence between specific classes of perturbation patterns and corresponding components of the induced β tensor belonging to the same irreducible representation of the symmetry group of the unsubstituted molecular backbone (exemplified here in the case of the D_{6h} group of

benzene). This procedure will be recognized as a general one, applicable to a broad range of molecular templates and substitution patterns. In Section V, quantum calculations along the lines defined in Section III are further simplified by means of a Singular Value Decomposition (SVD) of the linear operator which connects the 27 coefficients of the induced β with the on-site potential perturbation (6 terms for a full benzene substitution pattern). Such description, amounting to a reorganization of the input potential and the output β coefficients in terms of their irreducible components will be shown to introduce considerable simplification in the presentation and rationalization of results. Calculations performed in Sections VI and VII permit a test of the validity of the EIP model by comparison with full quantum calculations on actual substituted molecules while allowing an exploration of situations beyond the linear coupling limit.

II. INTERNAL POTENTIAL MODEL

The model developed here extends the one-dimensional scalar-like equivalent internal field (EIF) model[41,42] to multipolar systems. In extending the model, we continue to view the molecule as a skeleton to which electron-acceptor/electron-donor substituents have been attached. These substituents exert an effective potential on the skeleton which we will refer to as the internal potential. This internal potential perturbs the skeleton and accounts for the hyperpolarizability of the total, or "dressed", system. For instance, if we assume the system to be essentially one-dimensional, as in Oudar's restricted approach, then the internal potential can be viewed as the source of an internal electric field applied along the x axis, $F_x^{(int)}$. Under illumination, the skeleton experiences both this internal field, $F_x^{(int)}$, and the external electric field of the laser, $F_x^{(ext)}$, such that the total field applied to the skeleton is

$$F_x^{(tot)} = F_x^{(int)} + F_x^{(ext)} \tag{2}$$

The energy, W, of the skeleton in the total field of Eq. (2) is given by,

$$W = W_0 - \mu_x F_x^{(tot)} - \frac{1}{2}\alpha_{xx} F_x^{(tot)^2} - \frac{1}{3}\beta_{xxx} F_x^{(tot)^3} - \frac{1}{4}\gamma_{xxxx} F_x^{(tot)^4} \tag{3}$$

where W_0 is the energy of the skeleton in zero field, and μ, α, β and γ are the susceptibilities of the skeleton. The susceptibilities of the dressed system may be obtained by substituting Eq. (2) into Eq. (3),

$$\bar{W} = \bar{W}_0 - \bar{\mu}_x F_x^{(ext)} - \frac{1}{2}\bar{\alpha}_{xx} F_x^{(ext)^2} - \frac{1}{3}\bar{\beta}_{xxx} F_x^{(ext)^3} - \frac{1}{4}\bar{\gamma}_{xxxx} F_x^{(ext)^4} \tag{4}$$

$$\bar{\alpha}_{xx} = \alpha_{xx}; \bar{\gamma}_{xxxx} = \gamma_{xxxx} \tag{5}$$

$$\bar{\mu}_x = \alpha_{xx} F_x^{(int)} \tag{6}$$

$$\bar{\beta}_{xxx} = 3\gamma_{xxxx} F_x^{(int)} \tag{7}$$

(Throughout this paper, we will use a bar to denote properties of the dressed system, as compared to those of the skeleton.) In Eqs. (4)-(7), we assume a centrosymmetric skeleton, such that μ and β of the skeleton are both zero. We also ignore terms that are higher than linear order in $F_x^{(int)}$. This assumption of linear response with respect to the internal potential is discussed in more detail below.

Note that according to Eq. (5), the even rank tensors $\bar{\alpha}$ and $\bar{\gamma}$ are unchanged at first order in $F_x^{(int)}$. The odd-rank tensors $\bar{\mu}$ and $\bar{\beta}$ are both proportional to the internal field, $F_x^{(int)}$, with proportionality constants that depend only on properties of the skeleton. This model therefore predicts that the ratio $\bar{\beta}/\bar{\mu}$ will be the same for all chemical substitutions of a given skeleton. Furthermore, this ratio can be derived from the susceptibilities, α and γ, of the skeleton, leading to Eq. (1).

In order to generalize this model so as to allow for the description of multipolar systems, we must take into account the full tensor character of both the internal potential and the resulting hyperpolarizability. While retaining the view that the affect of the substituents can be accounted for by the application of an electrostatic potential to the skeleton, we use a more general expanded form for the internal potential,

$$V(r, \theta, \phi) = \sum_{j=0}^{\infty} \sum_{m=-j}^{j} E_m^j r^j Y_m^j(\theta, \phi). \tag{8}$$

(See Appendix C for a discussion of this form.) The $j = 1$ terms of Eq. (8) are equivalent to the application of a uniform electric field to the skeleton, with the coefficients E_m^j being the electric field expressed in spherical tensor notation. Although the j=1 term is sufficient for the one-dimensional model summarized above, multipolar systems require terms with $j \neq 1$, which can not be modeled as an internal electric field. An important illustration of this case is the octupolar substitution pattern of Fig. 1, which amounts to an internal potential corresponding to $j = 3$.

In Eq. (3), the energy of the skeleton is expanded as a power series in the total field. This may be generalized to the internal-potential model by expanding the energy as a power

series in the coefficients, E^j_m of Eq. (8),

$$\begin{aligned} W \;=\; & W_0 - \sum_{j,m} \mu^j_m E^j_m - \frac{1}{2} \sum_{j,j',m,m'} \alpha^{j,j'}_{m,m'} E^j_m E^{j'}_{m'} \\ & -\frac{1}{3} \sum_{\substack{j,j',m,m' \\ j'',m''}} \beta^{j,j',j''}_{m,m',m''} E^j_m E^{j'}_{m'} E^{j''}_{m''} \\ & -\frac{1}{4} \sum_{\substack{j,j',m,m' \\ j'',j''',m'',m'''}} \gamma^{j,j',j'',j'''}_{m,m',m'',m'''} E^j_m E^{j'}_{m'} E^{j''}_{m''} E^{j'''}_{m'''}, \end{aligned} \tag{9}$$

where μ, α, β, and γ are generalized susceptibilities of the skeleton, expressed in spherical tensor notation. (The equivalent expansion traditionally expressed in Cartesian tensor notation, does not display the rotational invariance features attached to the irreducible tensor representation and is therfore less convenient and amenable to physical considerations than the presently used formalism.) Indeed, those terms of Eq. (9) for which all j's are equal to 1 are equivalent to the expansion of Eq. (3), with the susceptibilities transformed from Cartesian to spherical tensor notation. Moreover, the generalized irreducible expansion in Eq. (9) sustains new relevant terms which are not included in the cartesian expansion in Eqs. (3)-(4). For multipolar systems, the internal potential has components with $j \neq 1$, and this introduces generalized susceptibilities[45] which do not occur when the energy is expanded in the presence of the sole electric field. The susceptibilities may then be defined in terms of energy derivatives, for example,

$$\gamma^{j,j',j'',j'''}_{m,m',m'',m'''} = \frac{1}{3!} \frac{\partial^4 W}{\partial E^j_m \partial E^{j'}_{m'} \partial E^{j''}_{m''} \partial E^{j'''}_{m'''}}. \tag{10}$$

By analogy to Eq. (2), the potential experienced by the skeleton is a sum of the external potential due to the laser, $(E^j_m)^{ext}$, and the internal potential due to the chemical substituents, $(E^j_m)^{int}$

$$E^j_m = \left(E^j_m\right)^{ext} + \left(E^j_m\right)^{int}. \tag{11}$$

As with Eq. (4), the susceptibilities of the dressed system may be obtained by substituting Eq. (11) into Eq. (9), and extracting the coefficient of the appropriate powers of $(E^j_m)^{ext}$. Terms that are linear in the external potential give the permanent electrostatic moments of the dressed system. For instance, the coefficients of $(E^1_m)^{ext}$, $(E^2_m)^{ext}$ and $(E^3_m)^{ext}$ yield the permanent dipole, quadrupole and octupole moments of the dressed system. Similarly, the susceptibilities with respect to an applied electric field are obtained from the coefficients

of the appropriate powers of $(E_m^1)^{ext}$. Just as in the one dimensional model of Eq. (4), we retain only up to linear terms with respect to the internal potential. This thereby provides a recipe for relating the properties of the dressed system to those of the skeleton and the internal potential. For example, to obtain the first hyperpolarizability, which is related to $\bar{\beta}^{1,1,1}_{m,m',m''}$, we extract the coefficient of $\left((E_m^1)^{ext}\right)^3$ and retain up to linear terms in $(E_m^j)^{int}$

$$\bar{\beta}^{1,1,1}_{m,m',m''} = \beta^{1,1,1}_{m,m',m''} + \frac{3!}{2!} \sum_{j,m'''} \gamma^{1,1,1,j}_{m,m',m'',m'''} \left(E^j_{m'''}\right)^{int}. \tag{12}$$

Note that in this expression, the j coefficient attached to the internal field $E^j_{m'''}$ is not constrained to $j = 1$ and can thus account for higher order non-vectorial perturbation schemes which are not amenable to the traditional cartesian field expansion with purely $j = 1$ terms. Eq. (12) is a generalization of Eq. (7) that allows for both a multipolar internal potential and includes all tensor components of the susceptibility. Eq. (12) may also be written as

$$\bar{\beta}^{1,1,1}_{m,m',m''} = \beta^{1,1,1}_{m,m',m''} + \sum_{j,m'''} \frac{\partial \beta^{1,1,1}_{m,m',m''}}{\partial \left(E^j_{m'''}\right)^{int}} \left(E^j_{m'''}\right)^{int}. \tag{13}$$

In the 1-D model of Eqs. (4)- (7), γ_{xxxx} can be related to the derivative of β_{xxx} with respect to the field along the x direction. So in the 1-D model, the optical γ is related to the derivative of the optical β with respect to electric field. In the multipolar model of Eq. (13), the derivative of β is related to the optical γ only when $j = 1$. For $j \neq 1$, the derivative in Eq. (13) corresponds to a generalized susceptibility.[45]

Eqs. (8)-(13) represent a formal generalization of the internal potential model to multipolar systems, providing a means for obtaining the properties of the dressed system from the properties of the skeleton and the internal potential. However, due to the large number of tensor components in both the internal potential and the generalized susceptibilities, it is useful to develop a systematic means, readily connected to symmetry reductions, to summarize the relevant relationships for particular skeletons.

A convenient representation of the internal potential is obtained by recognizing that the molecular energy is most sensitive to the value of the potential at the atoms. Indeed, for the quantum chemical models used in Sec. III, the Hamiltonian contains only the value of the potential at the atomic sites. The internal potential of Eq. (8) for the benzene skeleton can then be represented by its value at each of the six carbon atoms. These six degrees of

freedom may be arranged in vector form,

$$\mathbf{V} = (V_1^{int}, V_2^{int}, V_3^{int}, V_4^{int}, V_5^{int}, V_6^{int}), \tag{14}$$

where V_i^{int} is the the value of the potential, $V(r, \theta, \phi)$ of Eq. (8), at the i^{th} site. Since, in relating the properties of the dressed system to those of the skeleton, we retain only up to linear terms with respect to the internal potential, it is convenient to rewrite Eq. (13) in a manner that emphasizes this linear relationship. This may be done by arranging the tensor components of the susceptibility into a column vector. For instance, the 27 tensor components of the first hyperpolarizability may be arranged into a vector $\boldsymbol{\beta}$. Eq. (13) may then be written,

$$\bar{\boldsymbol{\beta}} = \boldsymbol{\beta} + \mathbf{L}\mathbf{V}, \tag{15}$$

where $\mathbf{L}$ is a matrix with elements defined as,

$$L_{i,j} = \frac{\partial \beta_i}{\partial V_j^{int}}. \tag{16}$$

Eq. (15) provides a linear relationship between the susceptibility of the dressed system and the internal potential. The linear response matrix, $\mathbf{L}$, is a function only of the skeleton, and completely specifies the linear response of the molecule. Below, we use quantum chemistry to calculate the matrix $\mathbf{L}$. For the benzene skeleton, $\mathbf{L}$ is a large 27 by 6 matrix and we will consider two ways to extract the relevant information. The first is an analysis based on the molecular symmetry of the skeleton. The second is singular value decomposition (SVD), a numerical approach that summarizes the information contained in $\mathbf{L}$.

III. QUANTUM CHEMICAL CALCULATIONS

In this section, the linear response matrix, $\mathbf{L}$ of Eq. (15), is calculated using three quantum chemical models, Hückel theory, PPP (Pariser-Parr-Pople) theory[46], and INDO (Intermediate Neglect of Differential Overlap) theory[47]. In all three models, the benzene molecule is taken to lie in the (x,y) plane with D_{6h} symmetry and bond lengths of 1.41Å and 1.10Å for the C-C and C-H bonds, respectively.

Both the Hückel and PPP models consider only the π electrons. The form of the π-electron Hamiltonian is,

$$H_{benzene} = \sum_{\mu} \epsilon_\mu n_\mu + \sum_{\mu \neq \nu, \sigma} t_{\mu,\nu} a_{\mu\sigma}^\dagger a_{\nu\sigma} + \sum_{\mu,\nu,\sigma} \frac{U_{\mu,\mu}}{2} n_\mu \left(n_\mu - 1\right)$$

$$+ \sum_{\mu \neq \nu} \frac{U_{\mu,\nu}}{2} \left(n_\mu - 1\right) \left(n_\nu - 1\right), \tag{17}$$

where $a^\dagger_{\mu\sigma}(a_{\mu\sigma})$ creates (destroys) an electron with spin σ in the p_z orbital on the μ^{th} carbon atom, $n_\mu = \sum_\sigma a^\dagger_{\mu\sigma} a_{\mu\sigma}$ is the number operator for electrons on carbon μ, ϵ_μ is the on-site energy, $U_{\mu,\mu}$ is the on-site Coulomb energy, $U_{\mu,\nu}$ is the intersite Coulomb energy, and the sums are over the six carbon atoms of benzene. Transfer matrix elements, $t_{\mu\nu}$, are included only between adjacent carbon atoms.

Hückel theory ignores Coulomb interactions between electrons and so includes only the first two terms of Eq. (17). The hyperpolarizability predicted by Hückel theory depends only on the molecular structure and the transfer integral, $t_{\mu,\nu}$, between adjacent carbons. Since the results will be compared to those of INDO theory, and the hyperpolarizability is sensitive to the energy of the lowest excited state, the Hückel transfer integral is set to -2.65eV. Using this value, the lowest optically allowed state obtained from Hückel theory agrees with that of INDO theory.

PPP theory includes Coulomb interactions between electrons via the last two terms of Eq. (17). The calculations presented here use the Ohno parameterization[48] for the electron-electron potential,

$$U_{\mu,\nu}[eV] = \frac{14.397}{\sqrt{\left(\frac{14.397}{11.26}\right)^2 + \left(r_{\mu\nu}[\mathring{A}]\right)^2}}. \tag{18}$$

The ground electronic state is obtained from Hartree-Fock theory, and the excited states are obtained from single-configuration interaction (S-CI) theory. The S-CI calculations include all molecular orbitals. The transfer matrix element, $t_{\mu\nu}$, between adjacent carbons is set to -2.52eV, such that the lowest optically allowed state agrees with that obtained from INDO theory.

INDO theory includes both σ and π electrons and includes Coulomb interactions between electrons. Unlike the above two models, the INDO model has been parameterized such that the Hamiltonian may be obtained for any organic molecular structure[47]. The electronic states are obtained in the same manner as for PPP theory. Hartree-Fock theory is used for the ground state and S-CI theory with a complete set of molecular orbitals is used for the excited states. Since INDO is parameterized for arbitrary organic structures, we also use INDO theory for the calculations on the substituted benzene molecules presented in Sec. VII.

The linear response matrix, $\mathbf{L}$ of Eq. (16), is obtained by adding the internal potential of Eq. (14) to the Hamiltonian,

$$H = H_{benzene} + \sum_{\mu} V_{\mu}^{int} n_{\mu}. \tag{19}$$

This is similar to a finite-field perturbation[43], but permits a more general non-dipolar internal potential. For Hückel and PPP theory, n_μ is the number operator for the p_z-orbital on the μ^{th} carbon atom. For INDO theory, we consider two possibilities for the number operator. The first is to use the number operator for just the p_z-orbital on the μ^{th} carbon, which is consistent with the orbital perturbation argument in Appendix A. The second choice is to use the number operator for the total number of valence electrons on the μ^{th} carbon, which corresponds to placing the entire atom in an electrostatic potential with value V_{μ}^{int}.

The hyperpolarizability, in Cartesian coordinates, is calculated using a sum over states expression[3]

$$\beta_{ijk} = \frac{1}{2} \sum_{\wp} \sum_{m,n \neq 0} \frac{\langle 0| \mu_i |n\rangle \langle n| \Delta\mu_j |m\rangle \langle m| \mu_k |0\rangle}{E_{0n} E_{0m}}, \tag{20}$$

where $|0\rangle$ is the Hartree-Fock ground state, $|m\rangle$ and $|n\rangle$ are S-CI excited states, $\Delta\mu_j = \mu_j - \langle 0 |\mu_j| 0\rangle$, E_{0m} is the difference in energy between the ground and excited states, and $\wp$ is a summation over all six permutations of the tensor indices. Eq. (20) is first evaluated in atomic units (energy in Hartrees, charge in units of e, and length in Bohr radii), and then multiplied by $8.6392 * 10^{-33}$ to convert to esu[49].

It is convenient to transform the Cartesian tensor of Eq. (20) to a spherical tensor representation. This is done via Clebsch-Gordon coefficients, as discussed in Ref. 27 and summarized in Appendix B. The norm of β is taken as,

$$\left|\beta^J\right| = \sqrt{\sum_M \left(\beta_M^J\right)\left(\beta_{-M}^J\right)} \;\; ; \;\; |\beta| = \sqrt{\sum_{J,M} \left(\beta_M^J\right)\left(\beta_{-M}^J\right)} = \sqrt{\sum_J \left|\beta^J\right|^2}, \tag{21}$$

where the sum is over all J and M. Due to Kleinmann symmetry[5,7], which is valid away from resonance, only the $J = 1$ and $J = 3$ components are non-zero.

The linear response matrix, $\mathbf{L}$, is obtained by numerical evaluation of the derivative in Eq. (16), using central differencing. The central difference is evaluated for each of the internal potential values, V_j^{int} of Eq. (14). For example, the derivative of the hyperpolarizability with respect to the first component of Eq. (14) is,

$$\frac{\partial \beta}{\partial V_1^{int}} = \frac{\beta(V_1^{int} = h) - \beta(V_1^{int} = -h)}{2h}, \tag{22}$$

where h is the step size and $\beta(V_1^{int} = h)$ is the first hyperpolarizability evaluated with an internal potential of magnitude h applied to site 1. A step size of $h = 0.001eV$ is used, which is sufficiently small that the first derivative of Eq. (22) is not contaminated by contributions from higher derivatives, yet is sufficiently large that numerical roundoff error is negligible.

IV. SYMMETRY ANALYSIS

The quantum chemical methods described above yield the linear response matrix, $\mathbf{L}$ of Eq. (15). For benzene, $\mathbf{L}$ is a 27x6 matrix, although since $\beta_{i,j,k}$ is symmetric with respect to permutation of indices, only 10 of the 27 components of β are unique. The first approach we will use to extract information from $\mathbf{L}$ is based on the molecular symmetry of the skeleton. In this approach, the tensors β and $\mathbf{V}$ are decomposed into components that transform as irreducible representations of the D_{6h} point group of the benzene skeleton. For substituted benzenes, β of the skeleton is zero and Eq. (15) becomes

$$\bar{\beta} = \mathbf{LV}. \tag{23}$$

Since $\mathbf{L}$ is a property of the molecular skeleton, it is invariant with respect to all symmetry operations of the bare skeleton. It therefore transforms as the totally symmetric representation, A_{1g}. The product $\mathbf{LV}$ then transforms according to the symmetry properties of $\mathbf{V}$, since $A_{1g} \otimes \Gamma = \Gamma$ for any symmetry representation Γ. Thus, application of an internal potential that transforms as symmetry representation Γ induces a hyperpolarizability that also transforms as Γ.

To create symmetry-adapted forms of the hyperpolarizability tensor, we first define a projection operator P^Γ that, when applied to a function, retains only that component of the function that transforms as the symmetry species Γ. In other words, P^Γ is the projection operator from the unrestricted tensor onto the irreducible subset Γ. It is convenient to work with spherical tensors, $\bar{\beta}^J_M$, such that the transformation properties of $\bar{\beta}^J_M$ are identical to those of the spherical harmonic Y^J_M. The projection operator P^Γ is defined by its action on $\bar{\beta}^J_M$ as,

$$P^\Gamma \bar{\beta}^J_M = \left(\frac{d^\Gamma}{h}\right) \sum_R \chi^\Gamma(R)(-1)^{inv*J} \sum_N D^J_{M,N}(R)\bar{\beta}^J_N, \tag{24}$$

where h is the order of the group, d is the degeneracy of the symmetry species Γ, R labels the symmetry operations of the point group, χ is the character for operation R in symmetry

species Γ, $D^J_{M,N}(R)$ is a coefficient of the Wigner operator associated with the operation R (Ref 50), and inv is 1 if R involves an inversion and zero otherwise. By applying the projection operator to each of the components, $\bar{\beta}^J_M$, we can determine all linear combinations of the $\bar{\beta}^J_M$ that transform as species Γ. The results are listed in Table I. A similar procedure yields the symmetry-adapted internal potentials of Table I. Note that, as expected, these symmetry-adapted potentials mirror the π-orbitals of benzene[51].

As was discussed above, since $\mathbf{L}$ of Eq. (23) transforms as the totally symmetric representation, A_{1g}, an acceptor-donor substitution pattern that causes the skeleton to experience an internal potential of symmetry Γ, within the linear response approximation, induces a hyperpolarizability of symmetry Γ in the dressed system. For example, an internal potential with B_{1u} symmetry, corresponding to the octupolar substitution pattern of Fig. 1(b), will induce a hyperpolarizability of B_{1u} symmetry, $\bar{\beta}^3_3 + \bar{\beta}^3_{-3}$. Comparison of the symmetry adapted internal potentials and hyperpolarizabilities reveals some general features. In Table I, only the B_{1u} and E_{1u} representations are present in both the symmetry-adapted hyperpolarizabilities and internal potentials. Although it is possible to form hyperpolarizabilities that transform as A_{2u}, B_{2u}, and E_{2u}, these will not arise from a linear response with respect to an internal potential applied to the carbon atoms of benzene. Similarly, the absence of g-symmetry hyperpolarizability tensors in Table I indicates that application of the g-symmetry internal potentials, A_{1g} and E_{2g}, will not induce a hyperpolarizability. This is as expected, since application of a g-symmetry internal potential does not remove the center of symmetry.

V. SINGULAR VALUE DECOMPOSITION

The symmetry analysis of the previous section reveals characteristic directions associated with the linear response matrix, $\mathbf{L}$. Another approach to extract information from the linear response matrix, $\mathbf{L}$, is via singular value decomposition (SVD). SVD is essentially the partial diagonalization of a rectangular matrix and it decomposes the 27x6 matrix, $\mathbf{L}$, into a product of three matrices

$$\mathbf{L} = \mathbf{U}\mathbf{T}\mathbf{W}^\dagger \tag{25}$$

where $\mathbf{U}$ and $\mathbf{W}^\dagger$ are unitary matrices with sizes 27x27 and 6x6 respectively. $\mathbf{T}$ is a 27x6 matrix that is zero except for the upper-left corner which contains a diagonal 6x6 matrix.

Eq. (15) may be rewritten in terms of the output of the SVD factorization as,

$$\bar{\beta} = \beta + \mathbf{U}\mathbf{T}\mathbf{W}^{\dagger}\mathbf{V}. \tag{26}$$

Eq. (26) can be interpreted as follows. The rows of $\mathbf{W}^{\dagger}$ give characteristic directions for the internal potential. A general internal potential $\mathbf{V}$ can be written as a linear combination of these characteristic directions. This is accomplished by the matrix multiplication, $\mathbf{W}^{\dagger}\mathbf{V}$, which returns a vector containing the projection of $\mathbf{V}$ onto the characteristic directions. The elements of the diagonal matrix $\mathbf{T}$ give the magnitude of the hyperpolarizability induced by an internal potential of unit magnitude applied along each of these characteristic directions. Finally, in the multiplication by $\mathbf{U}$, the columns of $\mathbf{U}$ give the distribution of the response among the various tensor components. In particular, application of an internal potential with a form equal to the i^{th} row of $\mathbf{W}^{\dagger}$ induces a hyperpolarizability with norm $T_{i,i}$ and hyperpolarizability components given by the i^{th} column of $\mathbf{U}$.

For the benzene skeleton, the characteristic directions for the internal potential are determined by symmetry, and the rows of $\mathbf{W}$ are identical to the symmetrized internal potentials of Table I. The columns of $\mathbf{U}$ indicate that application of a B_{1u} potential induces a hyperpolarizability of form $\bar{\beta}^3_3 + \bar{\beta}^3_{-3}$, just as in Table I. For an E_{1u} internal potential, the columns of $\mathbf{U}$ indicate that $\bar{\beta}^3_1 = -\bar{\beta}^{3*}_{-1}$ and $\bar{\beta}^1_1 = -\bar{\beta}^{1*}_{-1}$ (Appendix B shows that this is true in general). Note that B_{1u} potentials induce $m = 3$ components, while E_{1u} potentials induce $m = 1$ components. In addition, for an E_{1u} internal potential, the ratio of the norms of the J=1 and J=3 responses is 2. This results from the fact that an E_{1u} potential induces only $m = 1$ components and the fact that for a planar molecule, such as the benzene skeleton considered here, the ratio of $\left|\beta^1_{\pm 1}\right|$ to $\left|\beta^3_{\pm 1}\right|$ is 2 (Appendix B shows that this ratio applies to any planar molecule).

Table II shows the magnitude of the hyperpolarizabilities induced by B_{1u} and E_{1u} potentials, as given by the diagonal elements of $\mathbf{T}$ in Eq. (26). As expected, the diagonal elements of $\mathbf{T}$ are identical for $E^{(a)}_{1u}$ and $E^{(b)}_{1u}$. The three quantum chemical models are shown in order of increasing complexity. As we go from Hückel to PPP theory, we stay within a π electron model but add Coulomb interactions between electrons. Addition of Coulomb interactions has a large effect, reducing the B_{1u} response by 66% and the E_{1u} response by 92%. The large impact of Coulomb interactions indicates that Hückel theory is not sufficient for calculations on these systems. In going to INDO theory, we include the σ bonding network as well as

the π electrons. As discussed in Sec. III, there are two ways to apply an internal potential within INDO theory. The first is to apply the potential to the π orbitals only. For this case, the only difference between the INDO and PPP models is the explicit inclusion of the sigma electrons. This reduces the B_{1u} response by about 30% and the E_{1u} response by only 3%. Finally, Table II shows the results obtained when the internal potential is applied to both the σ and π electrons of the INDO model. Relative to the π electron potential, the B_{1u} and E_{1u} responses are lowered by 40% and 15%, respectively. The PPP and INDO models are thus in reasonable agreement.

The relative magnitude of the hyperpolarizability induced by B_{1u} and E_{1u} potentials will be of interest below. The ratio between the norm of the hyperpolarizabilities induced by B_{1u} and E_{1u} potentials is 3 for Hückel theory, 12 for PPP theory, 7 for INDO theory with the internal potential applied to only the π electrons and 5 for INDO theory with the potential applied to the entire atom. Since the INDO model is the most complete, we take the range 5 to 7 as a reasonable quantum chemical estimate of this ratio.

VI. NONLINEARITY WITHIN THE INTERNAL FIELD MODEL

Both the symmetry and SVD analyses assume linear response, such that the optical susceptibilities and other properties of the dressed system are linearly related to the internal potential (Eqs. (23) and (26)). In this section, we stay within the internal potential model, but consider breakdown in the linear response approximation. This is done by examining the hyperpolarizability as a function of the strength of the internal potential, with no reference to the linear expansion of Eqs. (15) and (16). The potential is applied along the symmetry-adapted directions of Table I. Note that internal potentials of *gerade* symmetry do not remove the center of symmetry, and so do not induce a hyperpolarizability.

Fig. 2 shows the norm of the hyperpolarizability induced by internal potentials applied in the B_{1u}, octupolar, symmetry direction. Table I indicates that the linear response with respect to this internal potential is of the form $\beta^3_3 + \beta^3_{-3}$. Fig. 2 indicates that this holds also for arbitrary strength internal potentials. This can be understood in terms of the symmetry of the perturbed system. Application of a B_{1u} internal potential reduces the symmetry of the system from D_{6h} to D_{3h}, and $\beta^3_3 + \beta^3_{-3}$ is the only third-rank tensor that transforms as the totally symmetric A'_1 representation of the D_{3h} point group. Hence, unlike the E_{1u}

case to be detailed below, nonlinearity resulting from strong internal potentials does not introduce new tensor components into the hyperpolarizability.

As expected from the results of the linear response analysis in Table II, the predictions from the Hückel model are substantially larger than those of the PPP or INDO models. For all three models, however, the response rises to a maximum between approximately 2.5 and 4eV. The hyperpolarizability increases nearly linearly with internal potential up to about 2eV, corresponding to an internal potential with magnitude 0.8eV alternating from atom to atom according to the internal potential of Table I. This places the validity of the linear response regime at about 0.8eV applied to each atom, or equivalently, a difference of 1.6eV in the potential applied to adjacent carbon atoms.

The existence of a maximum in Fig. 2 may be rationalized by analogy to a similar behavior seen in push-pull polyenes[52]. In those systems, increasing the strength of the acceptors and donors enhances the change in permanent dipole moment upon excitation to the charge-transfer states, while simultaneously decreasing the transition moments to these states. Since these two factors have opposing effects on the hyperpolarizability, a maximum response is obtained for an intermediate acceptor-donor strength. Although there is no permanent dipole moment for the ground and excited states of a benzene perturbed with a B_{1u} potential, it seems likely the maximum still results from a balance between the amount of charge being displaced on excitation and the transition moment to these charge-displaced states. This effect had been noted previously for planar octupolar molecules in Ref. 13.

The hyperpolarizability induced by an internal potential with E_{1u} symmetry is shown in Figs. 3 and 4. The total magnitude of the response is shown in Fig. 3. In the linear response analysis of Table II, the hyperpolarizability predicted by Hückel theory is a factor of 12 larger than that of PPP or INDO theory. Fig. 3 shows that this discrepancy becomes even larger for strong potentials. Apparently, inclusion of electron-electron interactions has a large effect on the predicted hyperpolarizability and so Hückel theory is not adequate for calculations on these systems.

Fig. 4 shows the various tensor components of the hyperpolarizability induced by an E_{1u} internal potential. The slopes near zero potential are as expected from the linear response results in Table II. For the m = 1 components that are allowed in linear response, $\beta^3_{\pm 1}$ and $\beta^1_{\pm 1}$, the linear regime extends to about 5eV. The dominant nonlinear effect is the appearance of m = 3, $\beta^3_{\pm 3}$, components. Although these are not allowed in linear response, they grow

in nonlinearly[53] and become comparable to the other components above about 2eV. At this magnitude, the carbon atoms at opposite sides of the benzene ring differ in potential by up to 2eV.

VII. INDO CALCULATIONS ON SPECIFIC CHEMICAL ACCEPTOR AND DONOR SUBSTITUENTS

This section reports INDO calculations for a variety of acceptor/donor substitution patterns on the benzene skeleton. The molecular geometries were optimized with the AM1 Hamiltonian[54], and the hyperpolarizabilities were calculated from INDO theory, with external fields modelled as in Eq. (19) (see Sec. III).

A. Hyperpolarizabilities

Tables III and IV show the norm of the hyperpolarizability for a variety of substitution patterns on the benzene skeleton, which we will examine in light of the above analysis. Table III compares *mono*-substituted species with disubstituted species, for both *ortho* and *meta* substitution. Para substitution is not included, since such systems have a center of symmetry and so have no hyperpolarizability.

For a planar molecule, the norm of the $(J = 1, m = 1)$ components is predicted to be twice that of the $(J = 3, m = 1)$ components, $\left|\beta^1_{\pm 1}\right| / \left|\beta^3_{\pm 1}\right| = 2$. This ratio is observed for all molecules in Table III, except those involving methyl substituents and *meta*-dinitrobenzene, since the interaction between the *meta* NO_2 substituents causes them to rotate out of plane.

We will begin by considering how the results obtained above regarding the different effects for B_{1u} versus E_{1u} internal potentials apply to the molecules in Tables III and IV. Table I indicates that a basic difference between these internal potentials is that, within the regime where the hyperpolarizability depends linearly on the internal potential, a B_{1u} potential induces only $m = 3$ components, $\beta^3_{\pm 3}$, while an E_{1u} potential induces only $m = 1$ components, $\beta^3_{\pm 1}, \beta^1_{\pm 1}$. Assuming that a substituent alters the internal potential on only the carbon atom to which it is attached, the internal potentials of the various substitution patterns can be written as linear combinations of the symmetry-adapted potentials of Table I. For instance, a unit internal potential for *mono*-substituted benzene can be written in the

vector notation of Table I as $V_{mono} = [1,0,0,0,0,0]$. This potential can be expanded as

$$V_{mono} = \frac{1}{\sqrt{6}}A_{1g} + \frac{1}{\sqrt{3}}E_{1u}^{(a)} + \frac{1}{\sqrt{3}}E_{2g}^{(a)} + \frac{1}{\sqrt{6}}B_{1u}. \tag{27}$$

Similarly, the di-substitutions lead to

$$V_{ortho} = \frac{1}{\sqrt{3}}A_{1g} + \sqrt{\frac{3}{8}}E_{1u}^{(a)} + \frac{1}{\sqrt{8}}E_{1u}^{(b)} + \frac{1}{\sqrt{24}}E_{2g}^{(a)} + \frac{1}{\sqrt{8}}E_{2g}^{(b)} \tag{28}$$

and

$$V_{meta} = \frac{1}{\sqrt{3}}A_{1g} + \frac{1}{\sqrt{24}}E_{1u}^{(a)} + \frac{1}{\sqrt{8}}E_{1u}^{(b)} + \frac{1}{\sqrt{24}}E_{2g}^{(a)} - \frac{1}{\sqrt{8}}E_{2g}^{(b)} + \frac{1}{\sqrt{3}}B_{1u}. \tag{29}$$

The *gerade* internal potentials are centro-symmetric and so do not induce a hyperpolarizability. The hyperpolarizability then depends only on the relative magnitudes of the two *ungerade* configurations. Eqs. (27),(28) and (29) reveal that *ortho* substitution corresponds to application of a pure E_{1u} internal potential while *mono* and *meta* substitution corresponds to application of a mix of E_{1u} and B_{1u} internal potentials.

The *ortho* substitution pattern corresponds to a pure E_{1u} internal potential and, assuming linear response, an E_{1u} potential leads to a hyperpolarizability with only $m = 1$ components (see Table I). However, Fig. 4 indicates that $m = 3$ components arise from nonlinear coupling effects. The magnitude of the $m = 3$ components for the *ortho*-substituted species in Table III then provide a measure of the degree of nonlinearity present in those systems. For most *ortho* substituents in Table III, the m=3 components are two orders of magnitude smaller than the m=1 components, indicating that the nonlinearity is quite small. However, for the nitro substituent, the m=3 components are nearly 10% those of the m=1 components, and for the cyano substituent, the m=3 and m=1 components have similar magnitudes. This suggests that the strength of the nitro and cyano groups is sufficient to induce significant nonlinear coupling effects.

We next consider another convenient means of comparing the *mono*-substituted and disubstituted molecules of Table III. Within linear response, the effects of the internal potential are additive. Therefore, the *ortho*-substitution can be considered as the sum of a [1,0,0,0,0,0] internal potential and a [0,1,0,0,0,0] internal potential. Since these two potentials are related by a 60^o rotation about the C_6 symmetry axis of the benzene skeleton, their contributions to the hyperpolarizability can be modeled by rotating the hyperpolarizability of the *mono*-substituted system by 60^o and adding the resulting tensor to the original, unrotated tensor. For rotation by an angle ϕ about the C_6 symmetry axis, the tensor

components transform as $e^{im\phi}$. For m=1, this is equivalent to the transformation properties of a vector, and so we may use vector addition to determine the expected ratio between disubstituted and *mono*-substituted species. Addition of two unit-vectors with a 60^o angle between them yields a vector of length $\sqrt{3}$. Therefore, within linear response, the ratio of the m=1 components of the hyperpolarizabilities for *ortho*− and *mono*−substituted species, $|\beta^{(J)}_{\pm 1}|_{di}/|\beta^{(J)}_{\pm 1}|_{mono}$, should be about 1.7. This it true to within about 10% for all substituents except cyano and nitro, which deviate from 1.7 by up to 70%. These are the same two substituents that showed significant nonlinear effects, as measured above by the magnitude of the $m = 3$ components present in *ortho* substitution.

The *meta* disubstituted species may be treated in a manner similar to that of the *ortho* disubstituted species, but with a rotation of 120^o connecting the two contributing internal potentials, [1,0,0,0,0,0] and [0,0,1,0,0,0]. Addition of two unit vectors with a 120^o angle between them yields a vector of length 1. Therefore, within linear response, the ratio of the m=1 components of the hyperpolarizabilities for *meta*− and *mono*−substituted species, $|\beta^{(J)}_{\pm 1}|_{di}/|\beta^{(J)}_{\pm 1}|_{mono}$, should be be about 1. This is true to within about 15% for all substituents except cyano and nitro, again confirming that these substituents lead to significant nonlinear effects.

The m=3 components of the hyperpolarizability transform as $e^{i3\phi}$ with respect to rotation about the C_6 symmetry axis. The 60^o rotation associated with *ortho* substitution therefore leads to an exact cancellation of the $m = 3$ components of the hyperpolarizability. This is consistent with the lack of a B_{1u} component in the internal potential of Eq. (28) and the resulting lack of $m = 3$ components in linear response discussed above. For the 120^o rotation associated with *meta* substitution, the m=3 components of the hyperpolarizability add constructively, such that the norm of the m=3 components of the hyperpolarizability, $|\beta^{(3)}_{\pm 3}|_{di}/|\beta^{(3)}_{\pm 3}|_{mono}$, should be 2 for linear response. The observed ratios are within 10% of this value for most substituents. As expected based on previous measures of nonlinearity, the deviation is larger for cyano and nitro. Somewhat surprisingly, given the linear behavior obtained above for this substituent, the amino substitution deviates by the largest amount, 37%.

For the trisubstituted species of Table IV, the internal potential can be considered as arising from the addition of [1,0,0,0,0,0], [0,0,1,0,0,0], and [0,0,0,0,1,0]. These contributions are related by 120^o rotations, and the summation causes the m=1 components to cancel.

The lack of m=1 components is a general consequence of the D_{3h} symmetry of the dressed system and so applies even in nonlinear order (see Sec. VI). While the m=1 components cancel, the m=3 components add constructively, such that the ratio between $\beta^{(3)}_{\pm 3}$ of the *tri*- and *mono*-substituted species should be about three. For all substituents except cyano and nitro, the observed ratio in Table IV is 10 to 20% larger than three, indicating a super-linear behavior. For the cyano and nitro substituents, which exhibited significant nonlinear effects in the above analyses, the ratio is about 25% smaller than three, indicating a sub-linear behavior.

The above analysis compares the hyperpolarizability tensors obtained for different substitution patterns. This serves as a test of the additivity implicit in the assumption that the hyperpolarizability is linearly related to the internal potential. Here, we consider the relative magnitude of the m=3 and m=1 components. As discussed in Sec. IV, a B_{1u} internal potential induces m=3 tensor components, while an E_{1u} internal potential induces m=1 tensor components. In addition, the SVD analysis of Table II indicates that, assuming linear response within the INDO method, a B_{1u} potential induces a hyperpolarizability that is 5 to 7 times larger than an E_{1u} potential of equivalent magnitude. This, combined with the decompositions of Eqs. (27)- (29) allows us to predict the relative magnitude of the m=3 and m=1 tensor components of the hyperpolarizability. For the *mono*-substitution potential of Eq. (27), the ratio between the B_{1u} and E_{1u} components is $1/\sqrt{2}$. Since the SVD analysis predicts that the B_{1u} potential is 5 to 7 times more effective at inducing a hyperpolarizability, the ratio between the m=3 (B_{1u}) and m=1 (E_{1u}) components is predicted to be between 3.5 and 5. However, the observed ratios in Table III are between 0.73 and 1.36. This indicates that the E_{1u} potential is much more effective at inducing a hyperpolarizability than suggested by the SVD analysis. A similar result is obtained for *meta* substitution, where the ratio between the m=3 (B_{1u}) and m=1 (E_{1u}) components is predicted to lie between 7 and 10, while the ratios observed for the various *meta*-substituted benzenes in Table III lie between 1.7 and 2.7. Once again, an E_{1u} internal potential appears to induce a larger hyperpolarizability, relative to B_{1u}, than is suggested by the SVD analysis.

B. Permanent Moments

In the 1-D model of Eqs. (6) and (7), application of an internal electric field to the molecular skeleton induces both a permanent dipole moment and a hyperpolarizability. The ratio of these two quantities is then a constant that depends only on the skeleton. Here, we consider the extension of this relation to multipolar systems, by comparing the permanent moments of the benzene skeleton with the hyperpolarizabilities.

In calculating the permanent moments, we consider only the charges due to the π electrons of the benzene skeleton, since it is the π system that dominates the hyperpolarizability. The octupole moment of the π electron distribution is first calculated in Cartesian coordinates,

$$\mathbf{O}_{i,j,k} = \sum_A \frac{5}{2} q_A r_{i,A} r_{j,A} r_{k,A} \tag{30}$$

where r_A is the position of the A^{th} atom with Cartesian components $r_{i,A}$, and q_A is the charge of the π electron distribution on the A^{th} atom. This Cartesian tensor is then transformed into spherical tensor notation using the same method as was used in Sec. III. The resulting octupole has both J=1 and J=3 components. The traceless form of the octupole moment,

$$\mathbf{O}_{i,j,k} = \sum_A q_A \left\{ \frac{5}{2} r_{i,A} r_{j,A} r_{k,A} - \frac{1}{2} |r_A|^2 \left(\delta_{i,j} r_{k,A} + \delta_{i,k} r_{j,A} + \delta_{j,k} r_{i,A} \right) \right\} \tag{31}$$

where $\delta_{i,j}$ is the Kronecker delta function, leads to identical results for the J=3 components, but the J=1 components of the traceless octupole are identically zero.

In the internal potential model, the permanent moments of Eq. (30) and the hyperpolarizability are due to the same internal potential and so should be correlated with one another. To examine this correlation, a large set of substituted benzene molecules were generated, consisting of the 714 unique ways to arrange up to three of the substituents (OH, NH_2, CH_3, OCH_3, F, NO_2, and CN) around benzene. Fig. 5 shows the correlation between $|\beta^{(3)}_{\pm 3}|$ and $|\mathbf{O}^{(3)}_{\pm 3}|$. When all 714 molecules are included, the correlation is rather weak, R=0.54. The results of Sec. VII A suggest that the nitro and cyano substituents are strong, such that the relation between the hyperpolarizability and the internal potential is outside the linear response regime. Here, the strength of each substituent is investigated by examining the correlation obtained when all molecules containing that substituent are removed from the data set. Removal of all molecules containing a nitro substituent (the crosses of Fig. 5) leaves 467 molecules and raises the correlation from 0.54 to 0.81. A similar removal of each

of the other substituents has little effect on the correlation. Continuing in this manner, we begin with the 467 molecules remaining after removal of the nitro substituent, and remove all molecules containing a cyano substituent (the dots of Figs. 5 and 6). This leaves 285 molecules and raises the correlation to 0.91. Continuing removal of substituents has less effect on the correlation coefficient. Removal of molecules containing NH_2 (the stars of Figs. 5 and 6) leaves 158 molecules (the squares of Figs. 5 and 6) with a correlation of 0.97. That molecules with nitro and cyano substituents show the weakest correlation is consistent with the finding in Sec. VII A that these substituents are outside of the linear regime.

Correlations between other properties were examined for the 285 molecules that do not contain the cyano or nitro groups. Unlike the strong 0.91 correlation between $|\beta^{(3)}_{\pm 3}|$ and $|\mathbf{O}^{(3)}_{\pm 3}|$, the correlation between $|\beta^{(3)}_{\pm 1}|$ and $|\mathbf{O}^{(3)}_{\pm 1}|$ is only 0.39 and that between $|\beta^{(1)}_{\pm 1}|$ and $|\mathbf{O}^{(1)}_{\pm 1}|$ is only 0.41. The correlation between $|\beta^{(1)}_{\pm 1}|$ and the permanent dipole is also weak, R=0.24.

VIII. DISCUSSION

This paper extends the one-dimensional "Equivalent Internal Field" (EIF) model of nonlinear optics to multipolar chromophores. In these models, acceptors and donors are viewed as perturbing the molecular skeleton to which they are attached and this allows the properties of the substituted molecule to be related to those of the molecular skeleton. The extension from one to three dimensions requires two generalizations to the model. First, the equivalent internal field must be generalized to an equivalent internal potential. Second, all tensor components of the hyperpolarizability must be taken into account.

The internal potential model developed here assumes the hyperpolarizability and permanent moments are linearly related to the internal potential. Within this linear approximation, application of a symmetry-adapted internal potential induces a hyperpolarizability of the corresponding symmetry. For the benzene skeleton of Table I, two types of internal potentials, B_{1u} and E_{1u}, lead to non-zero hyperpolarizabilities. The hyperpolarizability induced by a B_{1u} potential has only $m = 3$ tensor components, while that induced by an E_{1u} potential has only $m = 1$ tensor components. The linear response of the skeleton may be further characterized through singular value decomposition (SVD). The SVD analysis yields all of the information extracted from the symmetry analysis, and in addition, predicts that a

B_{1u} potential will induce a hyperpolarizability that is 5 to 7 times larger in magnitude than that induced by an E_{1u} potential of equivalent magnitude. (Note that for a skeleton with less symmetry than benzene, an SVD analysis would provide significantly more information than a symmetry analysis alone.)

By applying internal potentials of increasing magnitude to the benzene skeleton, we can determine the point at which nonlinear effects become important (Figs. 2- 4). The results show that nonlinear effects become important when there is greater than about a 2eV difference between carbon atoms. In addition to altering the predicted magnitude of the hyperpolarizabilities, nonlinear effects can introduce new tensor components. For instance, application of an E_{1u} symmetry internal potential to benzene leads to only $m = 1$ tensor components in the linear regime, while nonlinear effects arising for strong internal potentials can lead to $m = 3$ components.

The series of substituted benzene molecules in Tables III- IV and Figs. 5- 6 test various predictions of the internal potential model. For the substituents F, CH_3, OCH_3, OH and NH_2, many of the predictions of the internal potential model apply. We will refer to these as weak, or linear, substituents. The substituents NO_2 and CN appear to be outside of the linear response regime, and we will refer to these as strong substituents. *Ortho* substitution corresponds to a pure E_{1u} potential and so, in the linear regime, should lead to hyperpolarizabilities with only $m = 1$ components. This is indeed seen for the weak substituents, while the strong substituents exhibit significant $m = 3$ components. The assumption of linear response also leads to specific predictions for the ratios between the hyperpolarizability induced by *mono-*, *ortho-* and *meta-* substitution on benzene. The predicted ratios differ for the $m = 1$ and $m = 3$ components, since these have very different transformation properties with respect to rotation about the C_6 axis of benzene. Again, the ratios predicted assuming a linear relation between the hyperpolarizability and internal potential are found to hold for the weak substituents but not for the strong substituents. Linear response also predicts that the various tensor components of the hyperpolarizability will be proportional to those of the permanent octupole moment of the molecular skeleton, and that the proportionality constant depends only on properties of the skeleton. For the ($J = 3$, $m = \pm 3$) components, the hyperpolarizability and permanent octupole are strongly correlated for molecules with weak substituents (Fig. 6). These results indicate that many of the predictions of the internal potential model hold for benzene molecules with weak substituents.

There are, however, two cases where the predictions of the internal potential model are not observed for benzene molecules with weak substituents. The first case is for predictions that rely on an estimate of the relative magnitude of the hyperpolarizability induced by a B_{1u} symmetry potential as compared an E_{1u} potential. In the SVD analysis of Sec. V, the hyperpolarizability induced by a B_{1u} symmetry potential was predicted to be 5 to 7 times larger than that for an E_{1u} potential of the same magnitude. Results for the substituted benzene molecules indicate that the hyperpolarizabilities induced by B_{1u} and E_{1u} potentials have roughly equal magnitudes. Linear response also predicts that the ratio between the $m = 1$ components of the hyperpolarizability and the $m = 1$ components of the permanent octupole moment should be a constant, whereas the correlation between these properties is only R=0.41.

For a one-dimensional system, Eq. (1) relates the hyperpolarizability to the permanent dipole moment of a system and properties of the molecular skeleton. This relation can be obtained by using the permanent moment to determine the magnitude of the equivalent internal field in the system, and then using this internal field to predict the hyperpolarizability. The generalization of this procedure to multipolar systems is to use the permanent octupole moment to obtain the equivalent internal potential, and then use this internal potential to predict the hyperpolarizability. The good correlation between the ($J = 3$, $m = \pm 3$) components of the octupole and hyperpolarizability for weak substituents in Fig. 6 indicates that this procedure will work well for these tensor components. However, poor correlation is seen for the other tensor components. The relation of Eq. (1) can therefore be generalized to multipolar molecules, such that the ($J = 3$, $m = \pm 3$) components of the hyperpolarizabity are proportional to the corresponding components of the permanent octupole moment, with a proportionality constant that depends only on the molecular skeleton.

In summary, the equivalent internal field model has been extended to multipolar chromophores and tested against explicit calculations on substituted benzene molecules. The results indicate that for weak acceptor-donor substituents, many of the predictions of the internal field model hold. It therefore provides a good starting point for a general analysis of the relationship between the large variety of substitution patterns possible for multipolar chromophores and the tensor components of the hyperpolarizability induced by these patterns. This model is currently being extended and applied to 3-D systems and even order tensors (α and γ hyperpolarizabilities).

APPENDIX A: QUANTUM CHEMICAL REPRESENTATION OF ACCEPTOR AND DONOR SUBSTITUENTS

In the model developed here, acceptor and donor substituents are viewed as applying an internal potential to the molecular skeleton. One rationale for this approach is to consider the substituent as perturbing the energy of the π orbitals through the carbon to which it is attached. This is shown schematically in Fig. 7.

For an electron donating substituent, the HOMO of the substituent interacts with the orbitals of the benzene ring. Since this orbital has an energy below the benzene π system, interactions raise the energy of the orbital on the carbon to which the substituent is attached. For an electron withdrawing substituent, the LUMO of the substituent has an energy above the benzene π system, and interactions lower the energy of the orbital on the carbon atom to which the substituent is attached. Since the interaction occurs with the π molecular orbitals, this suggests that the internal potential should be applied only to the p_z orbitals of the molecular skeleton. In Sec. V, results are presented with the potential applied to the atom as a whole and to just the p_z orbital.

APPENDIX B: TRANSFORMATION OF THIRD-RANK TENSORS FROM CARTESIAN TO SPHERICAL REPRESENTATION

The transformation of the hyperpolarizability from Cartesian to spherical tensor notation[27] is shown in Table V. The Table assumes the hyperpolarizability is nonresonant, such that Kleinman symmetry applies. Note also that $\beta^J_{-m} = (-1)^m \beta^{J*}_m$. For planar molecules, the only nonzero components are those with $m = \pm 3$ and $m = \pm 1$. Examination of Table V also indicates that, for planar molecules, $\beta^1_{\pm 1} = -2\beta^3_{\pm 1}$. Therefore, for a planar molecule, we expect a ratio of 2 between $\left|\beta^{J=1}_{m=\pm 1}\right|$ and $\left|\beta^{J=3}_{m=\pm 1}\right|$.

APPENDIX C: FORM OF THE INTERNAL POTENTIAL

This appendix discusses the form of the internal potential in Eq. (8). The general form for the solution of the Laplace equation in spherical coordinates may be written (see Eq. (3.61)

of Ref. 55),

$$V(r,\theta,\phi) = \sum_{j=0}^{\infty} \sum_{m=-j}^{j} \left[E_m^j r^j + B_m^j r^{-(j+1)} \right] Y_m^j(\theta,\phi) \tag{C1}$$

For observation points, r, outside of a charge distribution, the boundary condition at $r = \infty$ constrains the coefficients E_m^j to zero. This leads to the standard multipolar expansion, with the coefficients B_m^j specifying a point monopole ($j = 0$), dipole ($j = 1$), quadrupole ($j = 2$) and so on, located at the origin of the coordinate system.

Here, we are interested in the potential applied to a molecular skeleton by acceptor and donor substituents arranged around the periphery of the skeleton. The skeleton can then be viewed as surrounded by a spherical shell of charge, $[\rho(r,\theta,\phi); r_{min} < r < r_{max}]$. Inside this charge shell, $r < r_{min}$, the boundary conditions at $r = 0$ require the coefficients B_m^j to be zero, and Eq. (C1) becomes

$$V(r,\theta,\phi) = \sum_{j=0}^{\infty} \sum_{m=-j}^{j} E_m^j r^j Y_m^j(\theta,\phi) \tag{C2}$$

which is the form of Eq. (8). For an observation point within the shell of charge considered above, $[\rho(r,\theta,\phi); r_{min} < r < r_{max}]$, the expansion coefficients are given by,

$$E_m^j = \frac{4\pi}{(2j+1)} \int_{r_{min}}^{r_{max}} r^2 sin(\theta) dr d\theta d\phi \, \frac{Y_m^{j*}(\theta,\phi)}{r^{j+1}} \rho(r,\theta,\phi). \tag{C3}$$

* Electronic address: yaron@chem.cmu.edu

† Electronic address: zyss@lpqm.ens-cachan.fr

[1] H. S. Nalwa and S. Miyata, Nonlinear Optics of Organic Molecules and Polymers (CRC Press, 1997).

[2] M. G. Kuzyk and C. W. Dirck, Characterization Techniques and tabulations for Organic Nonlinear Optical Materials (Marcel Dekker, New York, 1998).

[3] D. S. Chemla and J. Zyss, Nonlinear Optical Properties of Organic Molecules and Crystals, vols. 1 and 2 (Academic Press, New York, 1987).

[4] J. Zyss, Nonlinear Optics: Materials, Physics and Devices (Academic Press, New York, 1994).

[5] B. Dick, G. Stegeman, R. Twieg, and J. Zyss, Chem. Phys. **245** (1999).

[6] M. Barzoukas, M. Blanchard-Desce, D. Josse, J. M. Lehn, and J. Zyss, Chem. Phys. **133**, 323 (1989).

[7] B. Robinson, L. Dalton, A. Harper, A. Ren, F. Wang, C. Zhang, G. Totorova, M. Lee, R. Aniszfeld, S. Garner, et al., Chem. Phys. **245**, 35 (1999).

[8] M. Alheim, M. Barzoukas, P. Bedworth, M. Blanchard-Desce, A. Fort, Z.-Y. Hu, S. Marder, J. Perry, C. Runser, M. Staehelin, et al., Science **271**, 335 (1996).

[9] W. Steier, A. Chen, S. Lee, S. Garner, H. Zhang, V. Shuanov, L. Dalton, F. Wang, A. Ren, C. Zhang, et al., Chem. Phys. **271**, 487 (1999).

[10] Y. Shi, C. Zhang, J. Bechtel, L. Dalton, B. Robinson, and W. Steier, Science **288**, 119 (2000).

[11] J. L. Oudar and D. S. Chemla, J. Chem. Phys. **66**, 2664 (1977).

[12] J. L. Oudar, J. Chem. Phys. **67**, 446 (1977).

[13] M. Joffre, D. Yaron, R. J. Silbey, and J. Zyss, J. Chem. Phys. **97**, 5607 (1992).

[14] S. Brasselet and J. Zyss, International Journal of Nonlinear Optical Physics and Materials **5**, 671 (1996).

[15] Y. K. Lee, S. J. Jeon, and M. Cho, J. Am. Chem. Soc. **120**, 10921 (1998).

[16] R. Terhune, P. Maker, and C. Savage, Phys. Rev. Lett. **14**, 681 (1965).

[17] P. Maker, Phys. Rev., A **1**, 923 (1970).

[18] S. Yaliraki and R. Silbey, J. Chem. Phys. **111**, 1561 (1999).

[19] K. Clays and A. Persoons, Phys. Rev. Lett. **66**, 2980 (1991).

[20] P. Kaatz and D. P. Shelton, J. Opt. Soc. Am. B **16**, 998 (1999).

[21] J. Zyss, Nonlinear Optics **1**, 3 (1991).

[22] J. Zyss, J. Chem. Phys. **98**, 6583 (1993).

[23] J. Zyss, T. C. Van, C. Dhenaut, and I. Ledoux, Chem. Phys. **177**, 281 (1993).

[24] J. Zyss and I. Ledoux, Chem. Rev. **94**, 77 (1994).

[25] C. Dhenaut, I. Ledoux, I. Samuel, J. Zyss, M. Bourgault, and H. L. Bozec, Nature **374**, 339 (1995).

[26] I. Ledoux, J. Z. C. I. I. C. Khoo, F. Simoni, and e. C. Umeton, Novel Optical Materials and Applications (Wiley Interscience, 1997).

[27] S. Brasselet and J. Zyss, J. Opt. Soc. Am. B **257**, 15 (1998).

[28] C. Andraud, T. Zabulon, A. Collet, and J. Zyss, Chem. Phys. **245**, 243 (1999).

[29] T. Brotin, C. Andraud, I. Ledoux, S. Brasselet, J. Zyss, M. Perrin, A. Thozer, and A. Collet, Chem. Mater. **8**, 890 (1996).

[30] T. Renouard, H. L. Bozec, S. Brasselet, I. Ledoux, and J. Zyss, Chem. Comm. p. 871 (1999).

[31] M. Blanchard-Desce, J. B. Baudin, L. Jullien, R. Lorne, O. Ruel, S. Brasselet, and J. Zyss, Optical Materials **12**, 333 (1999).

[32] G. Sumod, A. Nangia, M. Muthuraman, M. Bagieu-Beucher, R. Masse, and J. F. Nicoud, New Jour. Chem. **25**, 1520 (2001).

[33] J. Zyss, S. Brasselet, V. R. Thalladi, and G. R. Desiraju, J. Chem. Phys. **658**, 109 (1998).

[34] V. Thalladi, S. Brasselet, H. Weiss, D. Blaser, A. Katz, H. Carrell, R. Boese, J. Zyss, A. Nangia, and G. Desiraju, J. Am. Chem. Soc. **120**, 2563 (1998).

[35] I. Ledoux, J. Zyss, J. S. Siegel, J. Brienne, and J. M. Lehn, Chem. Phys. Lett. **172**, 440 (19990).

[36] C. Fiorini, F. Charra, J. M. Nunzi, I. Samuel, and J. Zyss, Opt. Lett. **20**, 2469 (1995).

[37] S. Brasselet and J. Zyss, Opt. Lett. **22**, 1464 (1997).

[38] A. Donval, S. Brasselet, P. Labbé, and J. Zyss, Unconventional Optical Elements for Information Storage, Processing and Communications (Kluwer, 2000).

[39] R. Piron, E. Toussarere, D. Josse, S. Brasselet, and J. Zyss, Opt. Lett. **25**, 1255 (2000).

[40] R. Piron, E. Toussaere, D. Josse, and J. Zyss, Appl. Phys. Lett. **77**, 2461 (2000).

[41] J. L. Oudar and C. S. Chemla, Opt. Comm. **13**, 10 (1975).

[42] D. S. Chemla, J. L. Oudar, and J. Jerphagnon, Phys. Rev. B **12**, 4534 (1975).

[43] J. Zyss, J. Chem. Phys. **71**, 909 (1979), **70**, 3341 (1979), **71**, 909 (1979).

[44] M. Cho, S. Y. An, H. Lee, I. Ledoux, and J. Zyss, J. Chem. Phys. **116**, 9165 (2002).

[45] A. D. Buckingham, E. Lippert, and S. Bratos, Organic Liquids: Structure, Dynamics and Chemical Properties (John Wiley and Sons, New York, 1978).

[46] I. Ohmine, M. Karplus, and K. Schulten, J. Chem. Phys. **68**, 2298 (1978).

[47] J. Ridley and M. Zerner, Theor. Chim. Acta **32**, 111 (1973).

[48] K. Ohno, Theor. Chim. Acta **2**, 219 (1964).

[49] D. P. Shelton and J. E. Rice, Chem. Rev. **94**, 3 (1994).

[50] C. G. Gray and K. E. Gubbins, Theory of molecular fluids: Volume 1: Fundamentals (Clarendon Press, Oxford, 1984).

[51] L. Salem, The molecular orbital theory of conjugated systems (W. A. Benjamin, New York, 1966).

[52] S. R. Marder, D. N. Beratan, and L.-T. Cheng, Science **252**, 103 (1991).

[53] I. Ledoux, I. Cazenobe, S. Brasselet, E. Toussaere, and J. Zyss (2000).

[54] M. J. S. Dewar, E. G. Zoebisch, E. F. Healy, and J. J. P. Stewart, J. Am. Chem. Soc. **107**, 3902 (1985).

[55] J. D. Jackson, Classical Electrodynamics, Second Edition (John Wiley and Sons, New York, 1975).

FIGURES

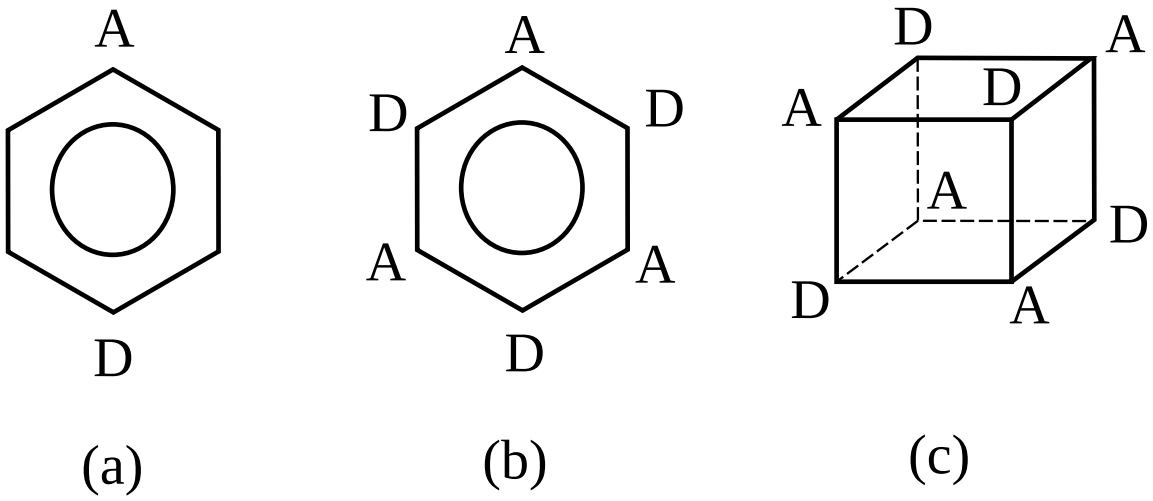

FIG. 1: Dipolar (a), 2-D octupolar (b), and 3-D octupolar (c) substitution patterns. A and D represent electron and donor substituents, respectively.

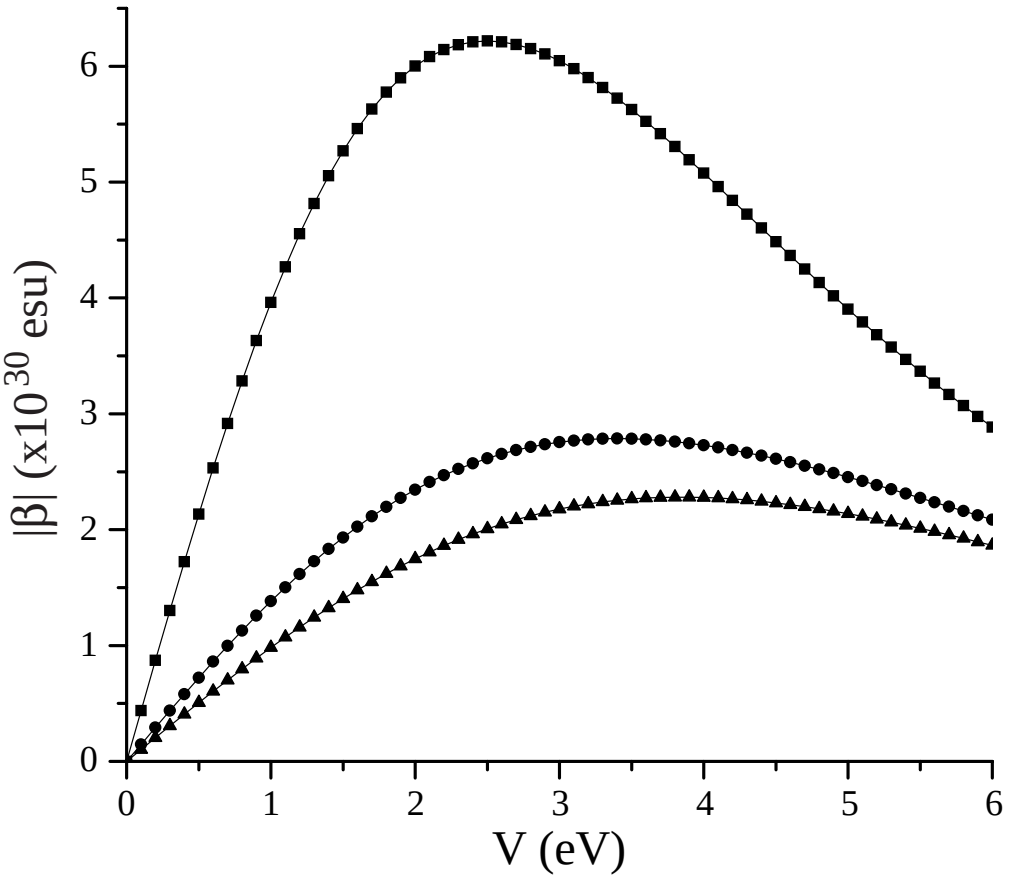

FIG. 2: Norm of the hyperpolarizability induced by an internal potential of B_{1u} symmetry for the Hückel (squares), PPP (circles), and INDO (triangles) models. V is the root mean square (RMS) magnitude of the potential. For all V, the hyperpolarizability tensor has B_{1u} symmetry, $\beta^3_3 + \beta^3_{-3}$.

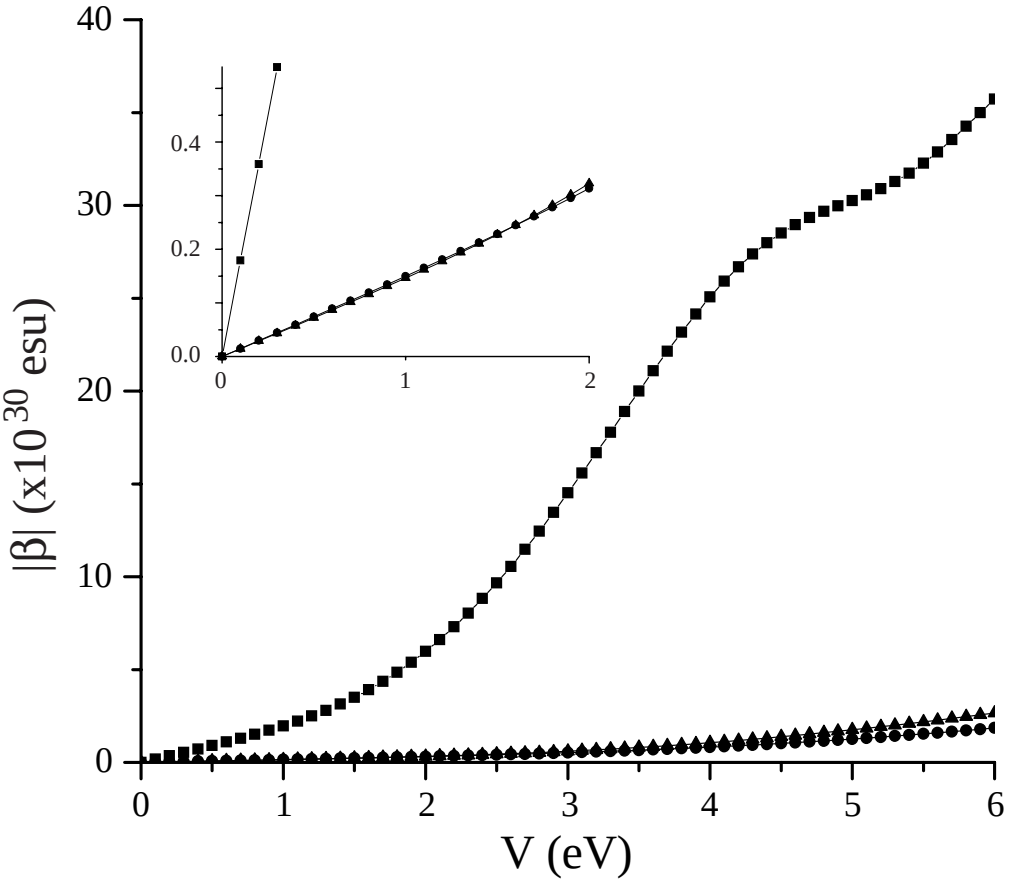

FIG. 3: Norm of the hyperpolarizability induced by an internal potential of E_{1u} symmetry for the Hückel, PPP, and INDO Models. The insert is a detail for small V, showing that the slopes near V=0 agree with the linear response results of Table II. Notation is as in Fig. 2.

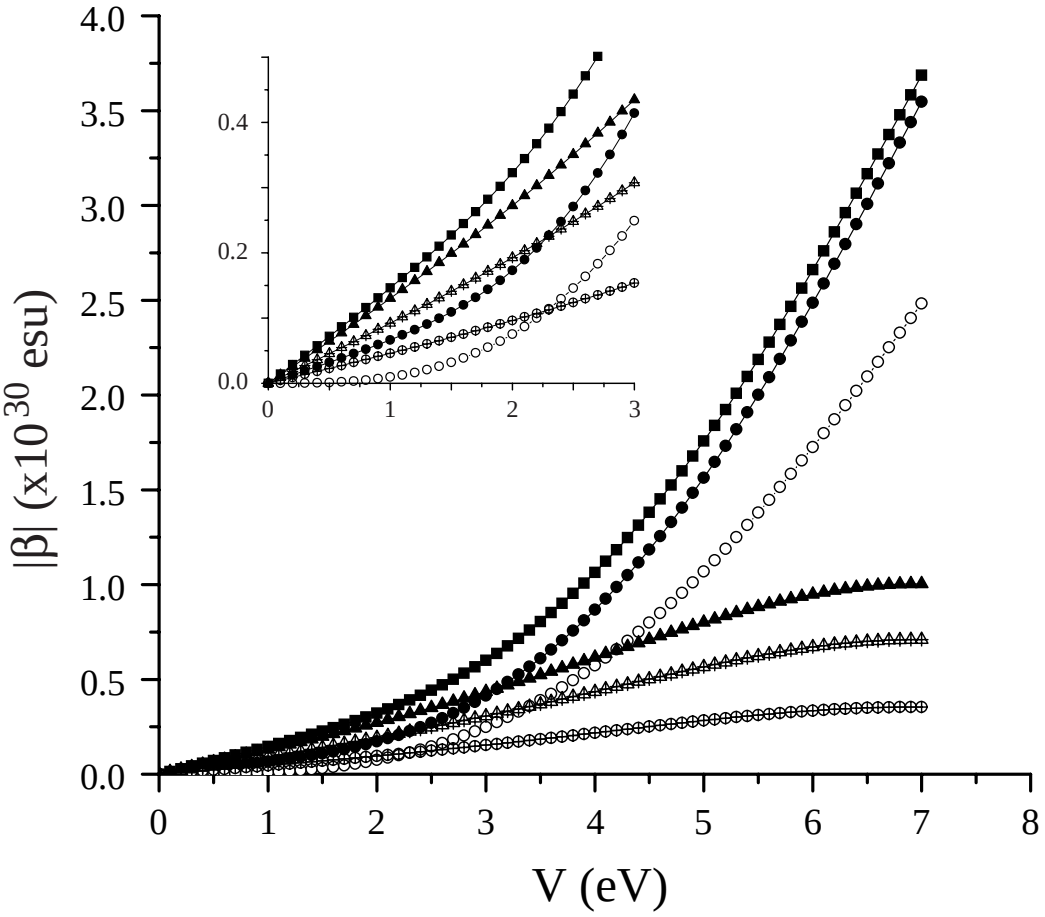

FIG. 4: Decomposition of the INDO results of Fig. 3 into its spherical tensor components. The insert is a detail for small V. Note that the $\beta^3_{\pm 3}$ component is zero in the linear response analysis, and here grows in quadratically with V. The filled squares are the total response, filled circles are the total $J = 3$ components, the empty circles are the $J = 3, m = 3$ components, the crossed circles are the $J = 3, m = 1$ components, the filled triangles are the total $J = 1$ components, and the crossed triangles the $J = 1, m = 1$ components.

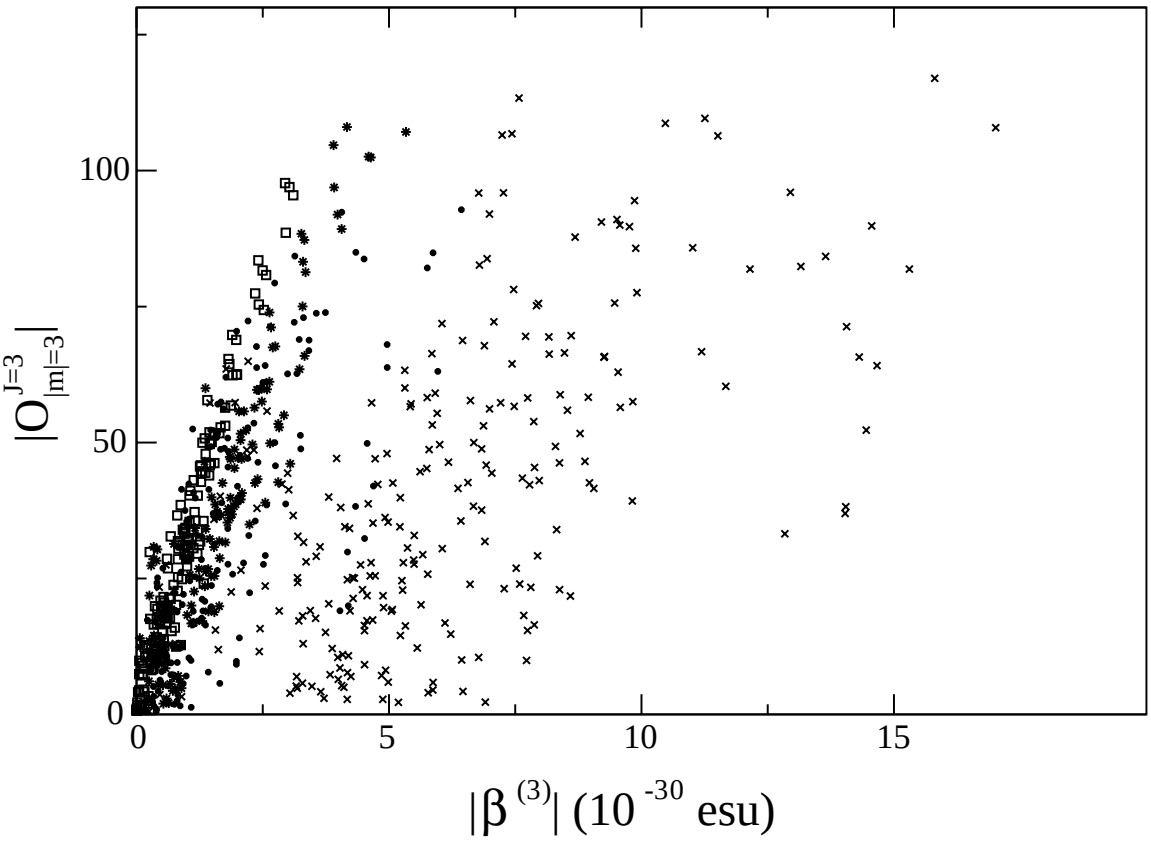

FIG. 5: $|\beta^{(3)}_{\pm 3}|$ versus $|\mathbf{O}^{(3)}_{\pm 3}|$ for the 714 molecules corresponding to the unique ways to arrange up to three of the substituents (OH, NH_2, CH_3, OCH_3, F, NO_2, and CN) on benzene. The correlation is R=0.54 for all molecules. Sequential removal of molecules containing NO_2 (x), CN (.), and NH_2 (*) raises the correlation to R=0.81, 0.91 and 0.97 respectively (see Sec. VIIB).

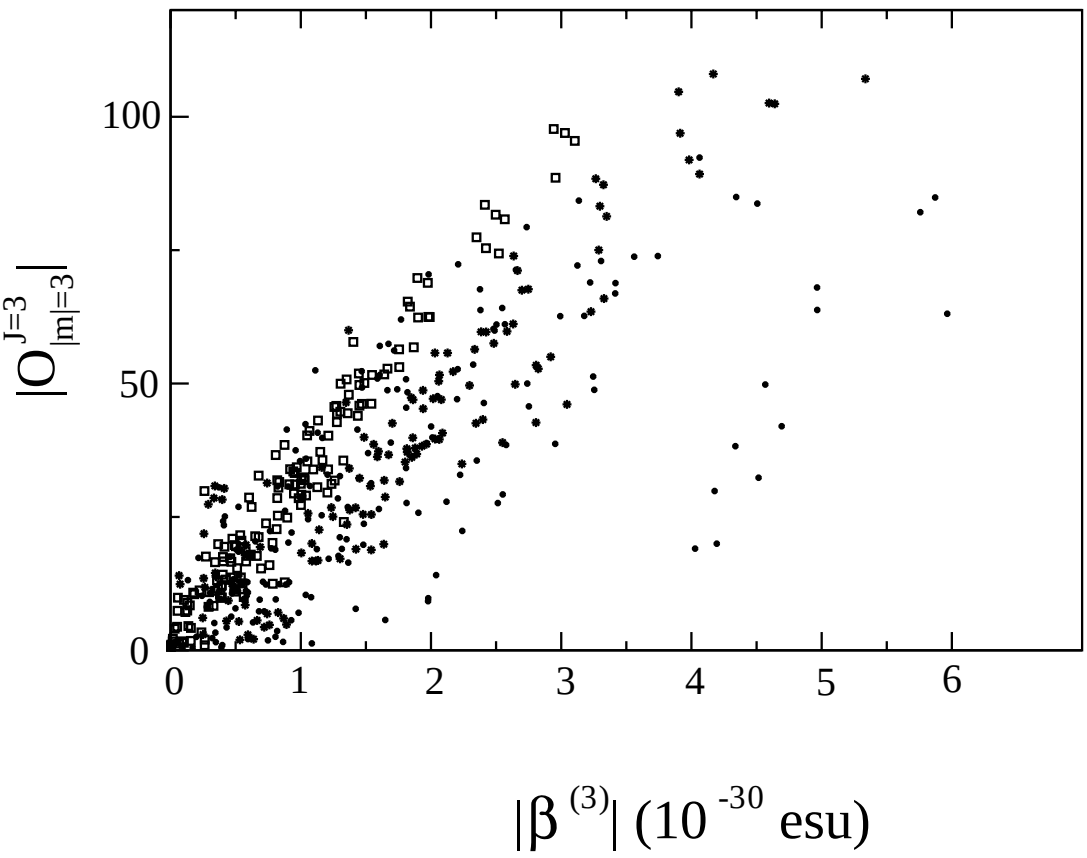

FIG. 6: The data of Fig. 5, with molecules containing NO_2 removed. The legend is as in Fig. 5.

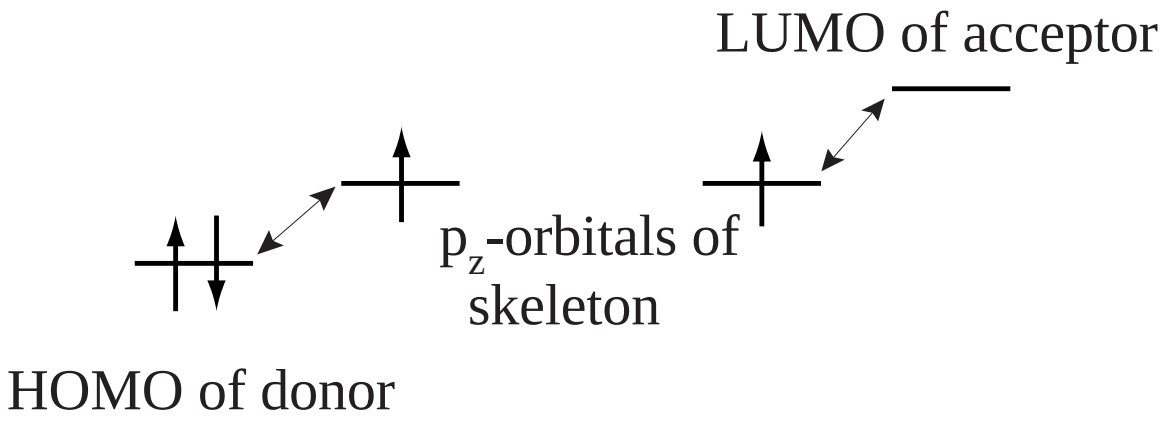

FIG. 7: Schematic representation of the effects of electron donor and acceptor substituents on a molecular skeleton. The HOMO of the donor substituent on the left interacts with the p_z-orbital of the skeleton, raising its energy. Similarly, the LUMO of the acceptor substituent on the right lowers the energy of the p_z-orbital on the carbon atom to which it is attached.

TABLES

TABLE I: Symmetry-adapted hyperpolarizability tensors and internal potentials for the D_{6h} point group of benzene. The notation $\{\bar{\beta}^3_1, \bar{\beta}^3_{-1}\}$ indicates that any linear combination of β^3_1 and β^3_{-1} will transform with the indicated symmetry. The internal potentials are given as a normalized vector representing the value of the potential on each of the six carbon atoms in benzene, $\mathbf{V}$ of Eq. (14). For the doubly-degenerate E groups, any unitary transformation of the two given vectors, $\mathbf{V}$, would be equally valid.

Symmetry	Hyperpolarizabilities		Internal Potentials
	J = 3	J = 1	
A_{1g}			$\frac{1}{\sqrt{6}}[1,1,1,1,1,1]$
A_{2u}	$\bar{\beta}^3_0$	$\bar{\beta}^1_0$	
B_{1u}	$\bar{\beta}^3_3 + \bar{\beta}^3_{-3}$		$\frac{1}{\sqrt{6}}[1,-1,1,-1,1,-1]$
B_{2u}	$\bar{\beta}^3_3 - \bar{\beta}^3_{-3}$		
$E^{(a)}_{2g}$			$\frac{1}{\sqrt{12}}[2,-1,-1,2,-1,-1]$
$E^{(b)}_{2g}$			$\frac{1}{2}[0,1,-1,0,1,-1]$
$E^{(a)}_{1u}$	$\{\bar{\beta}^3_1, \bar{\beta}^3_{-1}\}$	$\{\bar{\beta}^1_1, \bar{\beta}^1_{-1}\}$	$\frac{1}{\sqrt{12}}[2,1,-1,-2,-1,1]$
$E^{(b)}_{1u}$	$\{\bar{\beta}^3_1, \bar{\beta}^3_{-1}\}$	$\{\bar{\beta}^1_1, \bar{\beta}^1_{-1}\}$	$\frac{1}{2}[0,1,1,0,-1,-1]$
E_{2u}	$\{\bar{\beta}^3_2, \bar{\beta}^3_{-2}\}$		

TABLE II: Results of the SVD analysis on the benzene skeleton, using the quantum chemical models discussed in Sec. III. The values give the magnitude of the hyperpolarizability (in 10^{-30} esu's) induced by an internal potential of unit magnitude (in volts), along each of the symmetry directions in Table I. For the INDO model, results are shown with the internal potential applied to the entire atom and to just the π orbitals.

Model	B_{1u}	E_{1u}
Hückel	4.38	1.79
PPP, S-CI	1.47	0.148
INDO, S-CI,π orbitals only	1.02	0.143
INDO, S-CI, entire atom	0.615	0.121

TABLE III: Results from INDO calculations on *mono*- and *di*-substituted benzene molecules. $|\beta^{(J)}_{\pm m}|$ gives the magnitude of the individual tensor components (note that $|\beta^{(J)}_{m}| = |\beta^{(J)}_{-m}|$). $|\beta|$ is the norm of the hyperpolarizability and $|\beta_{(m)}|$ is the norm of all components with the indicated value of m. In the notation for substitution patterns, such as (X, H, H, H, H, H) for *mono*-substitution, the brackets enclose the substituents attached to each of the carbon atoms in order around the ring. The units for the hyperpolarizability are 10^{-30} esu.

mono-substituted, [X, H, H, H, H, H]

Substituent	$\lvert\beta\rvert$	$\lvert\beta^{(3)}_{\pm3}\rvert$	$\lvert\beta^{(3)}_{\pm1}\rvert$	$\lvert\beta^{(1)}_{\pm1}\rvert$	$\frac{\lvert\beta^{(1)}_{\pm1}\rvert}{\lvert\beta^{(3)}_{\pm1}\rvert}$	$\frac{\lvert\beta_{(m=3)}\rvert}{\lvert\beta_{(m=1)}\rvert}$
1) X = NO_2	6.55	3.73	1.22	2.45	2.01	1.36
2) X = CN	0.956	0.487	0.209	0.419	2.00	1.04
3) X = F	0.570	0.237	0.146	0.291	1.99	0.728
4) X = CH_3	0.614	0.292	0.178	0.266	1.49	0.912
5) X = OCH_3	1.45	0.653	0.355	0.705	1.99	0.827
6) X = OH	1.33	0.590	0.327	0.653	2.00	0.808
7) X = NH_2	2.52	1.06	0.643	1.28	1.99	0.740

ortho Disubstituted, [X, X, H, H, H, H]

Substituent	$\lvert\beta\rvert$	$\lvert\beta^{(3)}_{\pm3}\rvert$	$\lvert\beta^{(3)}_{\pm1}\rvert$	$\lvert\beta^{(1)}_{\pm1}\rvert$	$\frac{\lvert\beta^{(1)}_{\pm1}\rvert}{\lvert\beta^{(3)}_{\pm1}\rvert}$	$\frac{\lvert\beta_{(m=3)}\rvert}{\lvert\beta_{(m=1)}\rvert}$	$\frac{\lvert\beta^{(3)}_{\pm1}\rvert_{di}}{\lvert\beta^{(3)}_{\pm1}\rvert_{mono}}$	$\frac{\lvert\beta^{(1)}_{\pm1}\rvert_{di}}{\lvert\beta^{(1)}_{\pm1}\rvert_{mono}}$
1) X = NO_2	3.19	0.156	1.59	1.17	0.735	0.0790	1.30	0.477
2) X = CN	0.653	0.123	0.199	0.398	2.00	0.276	0.952	0.952
3) X = F	0.856	0.00553	0.271	0.542	2.00	0.00913	1.86	1.86
4) X = CH_3	0.822	0.0131	0.319	0.486	1.52	0.0225	1.79	1.83
5) X = OCH_3	2.21	0.0338	0.680	1.41	2.07	0.0216	1.91	2.00
6) X = OH	1.91	0.0786	0.604	1.21	2.00	0.0581	1.85	1.85
7) X = NH_2	3.29	0.00768	1.06	2.07	1.96	0.00330	1.65	1.62

meta Disubstituted, [X, H, X, H, H, H]

Substituent	$\lvert\beta\rvert$	$\lvert\beta^{(3)}_{\pm3}\rvert$	$\lvert\beta^{(3)}_{\pm1}\rvert$	$\lvert\beta^{(1)}_{\pm1}\rvert$	$\frac{\lvert\beta^{(1)}_{\pm1}\rvert}{\lvert\beta^{(3)}_{\pm1}\rvert}$	$\frac{\lvert\beta_{(m=3)}\rvert}{\lvert\beta_{(m=1)}\rvert}$	$\frac{\lvert\beta^{(3)}_{\pm3}\rvert_{di}}{\lvert\beta^{(3)}_{\pm3}\rvert_{mono}}$	$\frac{\lvert\beta^{(3)}_{\pm1}\rvert_{di}}{\lvert\beta^{(3)}_{\pm1}\rvert_{mono}}$	$\frac{\lvert\beta^{(1)}_{\pm1}\rvert_{di}}{\lvert\beta^{(1)}_{\pm1}\rvert_{mono}}$
1) X = NO_2	9.30	6.35	0.769	1.54	2.00	3.69	1.70	0.628	0.628
2) X = CN	1.22	0.843	0.0743	0.149	2.00	5.06	1.73	0.355	0.355
3) X = F	0.861	0.525	0.138	0.275	2.00	1.71	2.21	0.946	0.945
4) X = CH_3	0.964	0.607	0.191	0.243	1.27	1.96	2.08	1.08	0.913
5) X = OCH_3	2.21	1.41	0.308	0.614	1.99	2.05	2.16	0.867	0.871
6) X = OH	2.03	1.29	0.283	0.566	2.00	2.04	2.19	0.867	0.867
7) X = NH_2	4.53	2.91	0.592	1.19	2.01	2.19	2.75	0.920	0.933

TABLE IV: Results from INDO calculations on trisubstituted benzene molecules, using the notation of Table III. The only allowed tensor components for these systems are $\beta^{(3)}_{\pm 3}$.

	trisubstituted (X, H, X, H, X, H)		
Substituent	$\lvert\beta\rvert$	$\lvert\beta^{(3)}_{\pm 3}\rvert$	$\frac{\lvert\beta^{(3)}_{\pm 3}\rvert_{tri}}{\lvert\beta^{(3)}_{\pm 3}\rvert_{mono}}$
1) X = NO_2	11.7	8.27	2.22
2) X = CN	1.49	1.05	2.16
3) X = F	1.17	0.827	3.49
4) X = CH_3	1.40	1.00	3.39
5) X = OCH_3	3.18	2.25	3.44
6) X = OH	2.94	2.08	3.52
7) X = NH_2	5.45	3.85	3.64

TABLE V: Relation between the non-resonant hyperpolarizability expressed in Cartesian and spherical notation. The third column assumes a planar molecule lying in the (x,y) plane.

	non-planar	planar
β_0^1	$\frac{3}{\sqrt{15}}\left(\beta_{zzz}+\beta_{zxx}+\beta_{zyy}\right)$	0
$\beta_{\pm1}^1$	$\sqrt{\frac{3}{10}}\left[\mp\left(\beta_{xxx}+\beta_{xyy}+\beta_{xzz}\right)+i\left(\beta_{yyy}+\beta_{yxx}+\beta_{yzz}\right)\right]$	$\sqrt{\frac{3}{10}}\left[\mp\left(\beta_{xxx}+\beta_{xyy}\right)+i\left(\beta_{yyy}+\beta_{yxx}\right)\right]$
β_0^3	$\frac{1}{\sqrt{10}}\left[2\beta_{zzz}-3\left(\beta_{zxx}+\beta_{zyy}\right)\right]$	0
$\beta_{\pm1}^3$	$\frac{1}{2}\sqrt{\frac{3}{10}}\left[\pm\left(\beta_{xxx}+\beta_{xyy}\right)-4\beta_{xzz}-i\left(\beta_{yyy}+\beta_{yxx}\right)-4\beta_{yzz}\right]$	$\frac{1}{2}\sqrt{\frac{3}{10}}\left[\mp\left(\beta_{xxx}+\beta_{xyy}\right)+i\left(\beta_{yyy}+\beta_{yxx}\right)\right]$
$\beta_{\pm2}^3$	$\frac{3}{2\sqrt{3}}\left[\left(\beta_{zxx}-\beta_{zyy}\right)\mp2i\beta_{xyz}\right]$	0
$\beta_{\pm3}^3$	$\frac{1}{2\sqrt{2}}\left[\pm\left(-\beta_{xxx}+3\beta_{xyy}\right)+i\left(-\beta_{yyy}+3\beta_{yxx}\right)\right]$	$\frac{1}{2\sqrt{2}}\left[\pm\left(-\beta_{xxx}+3\beta_{xyy}\right)+i\left(-\beta_{yyy}+3\beta_{yxx}\right)\right]$